IN VITRO AND IN VIVO ASSESSMENT OF AMELOGENIN PEPTIDES COMPARED TO EMDOGAIN

A Thesis

By

THERESA ADRIA WORSHAM

Submitted to the Graduate and Professional School of Texas A&M University In partial fulfillment of requirement for the degree of

MASTER OF SCIENCE

Chair of Committee,	Xianghong Luan
Co-Chair	Thomas Diekwish
Committee Members,	Phillip Kramer
Head of Department	Matt Nair

May 2021

Major Subject: Oral Science

ABSTRACT

Objectives: To identify a cost-effective and well-defined alternative to currently available enamel matrix derivatives for periodontal regeneration.

Methods and Materials: For *in vitro* studies, human periodontal ligament cells (PDLCs) were treated with Emdogain (EMD), recombinant human AMEL isoforms rh174, rh163 and rh146 or synthetic amelogenin peptides sh147-163 and sh164-174 at a concentration of 10 □g/ml for 3, 7, 14 and 21 days on human periodontal ligament cells (PDLCs). Enamel protein function was assayed using wound healing and differentiation assays. For *in vivo* studies, collagen sponges (COL) were coated with human AMELs and EMD and implanted into C57 mouse skin subcutis or alveolar bone defects for 8 weeks, dissected and processed.

Results: Enamel protein derivative effects on PDLC differentiation fold-changes varied from 1.94(rh174), 1.4(rh163), 1.76(rh146)(amelogenin isoforms), 2.64(sh147-163) and 4.47(sh164-174)(amelogenin peptides), to 1.18(EMD). The two synthetic peptides shAMEL164-174 (10-fold versus EMD) and shAMEL147-163 (4-fold versus EMD) also proved more effective in terms of wound healing capacity. Subcutaneous collagen implants treated with sh164-174/Col, sh146-163/Col, EMD/Col and BSA/Col demonstrated migrated MSCs surrounded by new extracellular matrix in the sh164-174/Col and EMD/Col scaffolds while there were only individual cells in the sh146-163/Col and the BSA/Col scaffolds. MicroCT analysis revealed high bone volume to tissue volume ratios in the sh146-163 (0.42) and sh164-174 (0.44) groups versus 0.34 (periodontitis group), and 0.32 (EMD group), respectively. Histological assessment indicated that only sh164-174 treatment promoted mature bone formation and periodontal ligament reattachment to the tooth root, while the PDL remained delaminated in the EMD, sh146-163 and control groups.

Conclusion: When applied to periodontal defects in periodontitis animal models, shAMEL164-174 recruited mesenchymal stem cells, promoted periodontal ligament re-attachment and enhanced alveolar bone regeneration with superior effects on periodontal soft tissue wound healing and alveolar bone regeneration and without the effects of porcine EMD non-defined components.

ACKNOWLEDGEMENTS

I would like to thank my committee members, Dr. Luan, Dr. Diekwisch, and Dr. Kramer for their guidance and support throughout the course of this research. I would also like to thank my co-residents, colleagues, and the Department of Periodontics faculty and staff for making my time at Texas A&M University College of Dentistry a great experience and to allow me to grow as a clinician.

Finally, thanks to my family for their everlasting encouragement and support during this cumbersome venture. I could not have done it without them. This thesis is dedicated to all the people who helped me. You know who you are.

NOMENCLATURE

AI	amelogenesis imperfecta
ALP	alkaline phosphatase
BSA	Bovine serum albumin
TRAP	tyrosine-rich amelogenin peptide
PGA	propylene glycol alginate
EMD	enamel matrix derivative
cAMP	cyclic adenosine monophosphate
ALP	alkaline phosphatase
VEGF	vascular endothelial growth factor
Grp78	glucose-regulated protein 78
BMP	bone morphogenic proteins
PDLSC	periodontal ligament stem cells

CONTRIBUTORS AND FUNDING SOURCES

Contributors

This work was supervised by a thesis committee consisting of Professor Xianghong Luan and Professor Thomas Diekwish of the Department of Periodontics.

All work for the thesis was completed by the student, under the advisement of Xianghong Luan, Thomas Diekwish of the Department of Periodontics.

Funding Sources

There are no outside funding contributions to acknowledge related to the research and compilation of this document.

TABLE of CONTENTS

LIST OF FIGURES

LIST OF TABLES

1. INTRODUCTION AND LITERATURE REVIEW

Periodontal Wound Healing

During the acute phase of inflammation, the bacterial infiltration occurs and proinflammatory mediators are synthesized by the junctional epithelium which enter the connective tissue. These include interleukin (IL)-1, IL-8, prostaglandin E_2 (PGE_2), tumor necrosis factor-α (TNF-α) and matrix metalloproteinases (MMPs) (1). Following these chemotactic signals, gingival vessels are enlarged and facilitate the migration of neutrophils to the site of bacterial deposit. At the same time, the rate of turnover of the junctional epithelial cells increases, leaving widened spaces for neutrophil diffusion (*1*). Recruitment of neutrophils, proliferation of the epithelial cells and localized secretion of inflammatory enzymes and cytokines occur. These phenomena promote the subsequent recruitment of other inflammatory cells and destruction of the extracellular matrix.

During the late phase of immune response, small lymphocytes consisting of B and T cells infiltrate into the tissue in the presence of antigens and various cytokines. (2) B cells differentiate into plasma cells, producing antibodies against the invading pathogens. Macrophages are then activated through antigen non-specific mechanisms and enhance the overall inflammatory response by producing more inflammatory cytokines, including interferon γ, TNF-α, IL-1β, -6, -10, -12 and -15, PGE_2 and MMPs. Of these factors, IL-1β, TNF-α and PGE_2 are strongly implicated in the pathogenesis of periodontitis. An increase in inflammatory markers leads to lower expression and synthesis of collagen in fibroblasts, thus further assisting periodontal breakdown.

Amelogenin was thought to be expressed solely by ameloblasts during tooth development, however it has been found that this gene domain is also expressed in odontoblasts, cementoblasts

and other tissues suggesting amelogenins play a larger role in mesenchymal tissue growth (3-5). The only commercially available product on the market is Emdogain®; (Straumann AG, Basel, Switzerland). Which is labeled as an enamel matrix derivative (EMD). This product is derived from embryonal enamel of porcine origin. 90-95% of its composition are amelogenins, both long and short strands (6). To date, the only known active products are the amelogenins. The product is approved for periodontal regeneration. The original understanding of the enamel matrix derivative was that it recruited cementoblasts to the root surface while creating a stable hydrophilic surface for potential supporting interactions of cells to adjacent tissues. These interactions would lead to secondary regeneration of periodontal fibers and alveolar bone. However, multiple studies have now shown that amelogenins promote growth of multiple mesenchymal cells such as fibroblasts, osteoblasts and stem cells (3, 7, 8). Leading to the conclusion that amelogenins and or EMD can be used for other applications besides periodontal regeneration.

Amelogenin

Amelogenins are extracellular hydrophobic proteins derived from one gene. The structure and function of this extracellular protein family has been well evolutionary conserved. Amelogenins demonstrate a very high overall level of sequence homology among all higher vertebrates examined (>80%) (1). Amelogenin was thought to be expressed solely by ameloblasts during tooth development, however it has been found that this gene is also expressed in odontoblasts, cementoblasts and other tissues suggesting amelogenins play a larger role in mesenchymal tissue growth (2-4). Amelogenin plays a critical role in the structural organization of enamel as well as in mineralization. Mutations in gene expression can lead to diseases seen in

both humans and mice. Amelogenin gene mutations in humans and mice cause amelogenesis imperfecta (AI), one of the most common enamel genetic diseases (5).

The tyrosine amino- terminal and the hydrophobic carboxy- terminal ends of the amelogenin proteins affect its function and are important for mineralization. Amelogenins are saturated in proline residues, about 30%, and these resides actually hinder secondary structures such as beta sheets and alpha helixes from forming, creating a three dimensional structure of a nanosphere instead. The nanospheres self-assemble into a hydrophobic supramolecular matrix. During tooth development in the dental enamel organ this amelogenin matrix binds to hydroxyl apatite crystallites to structure the enamel matrix and to modulate the crystal growth (6). A sequenced protolytic process cleaves the amelogenin matrix slowly changing an insoluble hydrophobic matrix into a soluble matrix. This is part due to the carboxy-terminal being cleaved and absorbed back into the ameloblast. As enamel formation matures all of the amelogenin protein is removed and replaced with immature enamel crystallites to occlude and occupy the matrix space. The proteolytic process cleave amelogenin peptides then interact with other cell receptors. For example, TRAP, tyrosine-rich amelogenin peptide, is one candidate for an active peptide that can interact with cellular receptors (1). These active peptides will have an impact on wound healing which will be discussed later in the paper.

Current Therapeutic Strategies

The only commercially available product on the market is Emdogain®; Straumann AG, Basel, Switzerland. Which is labeled as an enamel matrix derivative (EMD). This product is derived from embryonal enamel of porcine origin. 90-95% of its composition are amelogenins, both long and short strands, the remaining products are proline-rich non-amelogenins, such as

tuftelin, tuft protein, ameloblastin, amelin and various serum proteins (7). To date, the only active products are the amelogenins. The product is approved for periodontal regeneration. The original understanding of the enamel matrix derivative was that it recruited cementoblasts to the root surface while creating a stable hydrophobic surface for potential supporting interactions of cells to adjacent tissues. These interactions would lead to secondary regeneration of periodontal fibers and alveolar bone. However, multiple studies have now shown that amelogenins promote growth of multiple mesenchymal cells such as fibroblasts, osteoblasts and stem cells (2, 8, 9). Leading to the conclusion that amelogenins and or EMD can be used for other applications besides periodontal regeneration.

For current clinical application of amelogenins, amelogenins are dissolved in an aqueous, acidic solution of propylene glycol alginate (PGA) in a gel formulation suitable for use in a syringe. When applied to a patient, the acidity of the gel is neutralized and the temperature increased, and amelogenins are released, undergo self-assembly and precipitate on the exposed tissue surfaces in the surgical area (1). During the healing phase of days and weeks the amelogenin is processed by matrix proteases and slowly release biologically active components into the surrounding environment, promoting regeneration and new growth.

Amelogenin first binds to cell surface receptors signaling a cyclic adenosine monophosphate (cAMP) response allowing uptake of amelogenin nanospheres. This response has been observed in periodontal ligament cells, blood cells, osteoblasts and murine ameloblasts (10). Amelogenin enhances the expression of tissue-specific markers such as alkaline phosphatase (ALP), collagen and osteocalcin in osseous tissues. These tissue-specific markers enhance maturation of cells such as fibroblasts, cementoblasts, osteoblasts and stem cells (10). Amelogenin has a cytostatic effect on osteoclasts and epithelial cells. This slight inhibitory effect

of epithelial cells gives collagen and other connective tissue cells the advantage of development and tissue repair.

The immunomodulatory effects of amelogenin induce the M2 macrophages. M2 stimulate cytokines such as IL-4 or IL-13 which are anti-inflammatory in nature. This induction of M2 macrophages creates a shift by changing gene expression from a pro-inflammatory to an anti-inflammatory environment. A recently discovered amelogenin binding protein, glucose-regulated protein 78 (Grp78) when bound enhances the proliferation of osteoblasts and the migration of periodontal ligament stem cells (PDLSC). This suggests a new therapeutic target for amelogenin-induced periodontal tissue regeneration (17). Stimulated M2 macrophages increase the production of VEGF which in turn plays an active role in angiogenesis (18).

EMD had both full length amelogenin molecules (7.4%) (17) and smaller amelogenin fragments. The full length amelogenin molecules have been shown to stimulate autocrine productions of bone morphogenic proteins (BMP). The smaller amelogenin fragments which consists of leucine rich amelogenin peptide (LRAP) and tyrosine-rich amelogenin peptide (TRAP) promote autocrine production of transforming growth factor (TGF)-β-like molecules (2). EMD stimulates the autocrine production of other growth factors such as vascular endothelial growth factor (VEGF), platelet-derived growth factors (PDGF) and cytokines like interleukin (IL)-6. In addition, other studies have shown that recombinant LRAP, presumably free of any mammalian growth factors, has obvious cell signaling activity (3).

Evaluating the gene expression on the effect of EMD on primary osteoblast revealed significant expression of more than 600 genes. The gene profile was similar to the bone-promoting parathyroid hormone (10). Amelogenin expression has been demonstrated in different long bone cells, in their precursor mesenchymal stem cells, in cartilage cells, and in specific cell

layers of the epiphyseal growth plate (11), suggesting that amelogenin has a role not only in enamel development but in development of many skeletal tissues. These studies demonstrate that amelogenins coordinate a sequenced array of growth factors that lead to regenerative effects.

Complete understanding and full use of amelogenin commercially available products such as Emdogain (EBD) has not been fully established yet. Its nanospheric hydrophobic self-assembled matrix structure provides a barrier for new growth to occur. Amelogenin enhances the expression of tissue-specific markers such as alkaline phosphatase (ALP), collagen and osteocalcin which enhance maturation of cells such as fibroblasts, cementoblasts, osteoblasts and stem cells, while also having a cytostatic effect on osteoclasts and epithelial cells to help create the ideal environment for new cell growth. The dynamic and well-orchestrated events of amelogenin on surrounding tissue has led to advancements in wound healing, post-operative pain, tissue regeneration and new tissue growth.

2. MATERIAL AND METHODS

Materials

Emdogain was obtained from Straumann (Switzerland). Recombinant human Amelogaenin (rhAMEL) fragments AMEL146, 163 and 174 were gifts from Dr. XXX. Small human AMEL peptides (shAMEL) were synthesized at Peptide2 (Chantilly, V). Collagen sponge Discs were purchased from Advanced BioMatrix (Carlsbad, CA). RhoA inhibitor, Rhosin, was obtained from Sigma (St Louis, MO).

Cell Culture

Periodontal ligament progenitor cells (PDLSCs) were isolated from human extracted third molars, and maintained in Dulbecco's modified Eagle's medium (Gibco BRL, Gaithersburg, MD, USA) supplemented with 10% fetal bovine serum (Atlanta Biologicals, Lawrenceville, GA, USA), 100 U/ml penicillin, 100 µg/mL streptomycin and 25 ng/ml Amphotericin B in a 5% CO_2 atmosphere at 37°C. Cell culture conditions were established by adding 10 µg/mL of EMD or Amelogenin derives to the culture medium. To study the effects of Amelogenin-derived fragments or small peptides on osteogenic differentiation, hPDLSC cells were subjected to a mineralization induction medium containing 10 nM dexamethasone, 50 µg/mL ascorbic acid and 2 mM β-glycerophosphate and cultured for 14 or 28 days. Upon terminating the culture, cells were subjected to alkaline phosphatase activity assays or alizarin red staining.

Hippo-YAP signal blocking using RhoA inhibitor or ITGb1 antibody

For inhibition of Hippo-Yap signaling, the anti-ITG b1 antibody (Abcam) or RhoA inhibitor (Sigma) was added to the cell culture medium at a concentration of 10mg/ml.

Cellular Motility Assay

A wound healing assay or a scratch assay is a laboratory technique used to study cell migration and cell–cell interaction. The assay was done by making a mechanical scratch on a cell monolayer and capturing images at regular intervals by time lapse microscope. It is specifically a 2D cell migration approach to semi-quantitatively measure cell migration of a sheet of cells. This scratch can be made through various approaches, such as mechanical, thermal, or chemical damage. The purpose of this scratch is to produce a cell-free area in hopes of inducing cells to migrate and close the gap.

The hPDL cells were grown to confluence on chamber slides. A linear scratch was made using a sterile 200uL pipette tip and the wells were washed three times with PBS. Twelve hours after the scratch, 10mg/ml EMD or AMEL derives was added to the cell cultures at different time points. The remaining wound area was measured using ImageJ software.

F-actin Analysis

After 24 hours of cell culture, cells were incubated with rhodamine phalloidin (Sigma) for 15 min at room temperature. Images were captured using a Zeiss LSM 710 microscope and analyzed by the CLSM image browser.

Alkaline phosphatase assay, alizarin red staining and light microscopy

Alkaline phosphatase (ALP) is a highly sensitive, simple, direct and HTS-ready colorimetric assay designed to measure ALP activity in serum and other mammalian samples. Alkaline Phosphatase also known as Basic Phosphatase catalyzes the dephosphorylation of many molecules including nucleotides and proteins. AP activity is high in pluripotent cells but is greatly decreased in more differentiated cell types. The technique described may be used to enumerate pluripotent cells during differentiation. It may also be used to monitor induced pluripotency using defined factors from more differentiated cell types.

Alizarin Red S, an anthraquinone derivative, may be used to identify calcium in tissue sections. The reaction is not strictly specific for calcium, since magnesium, manganese, barium, strontium, and iron may interfere, but these elements usually do not occur in sufficient concentration to interfere with the staining. Calcium forms an Alizarin Red S-calcium complex in a chelation process, and the end product is birefringent. This type of stain is used to detect bone.

To determine alkaline phosphatase (ALP) activity, control, EMD and AMEL derives-treated cells were washed and stained with alkaline phosphatase substrate (Roche Diagnostic, Indianapolis, IN). To determine mineralization potential, mineral deposits were detected after fixing with cold methanol and staining with 1% alizarin red solution. Phase-contrast images of control and treated hPDL cells were obtained using a Leica inverted microscope.

BRDU Incorporation Assay and Immunofluorescence Analysis

BrdU (Bromodeoxyuridine / 5-bromo-2'-deoxyuridine) is an analog of the nucleoside thymidine used in the BrdU assay to identify proliferating cells. BrdU can be incorporated into the newly synthesized DNA of replicating cells (during the S phase of the cell cycle during

which DNA is replicated). Antibodies specific for BrdU can then be used to detect the incorporated chemical thus indicating cells that were actively replicating their DNA.

The HistoMouse BRDU Kit (ThermoFisher) was used to detect BRDU incorporation (ab152095, Abcam). In brief, PDL cells were cultured in cell culture chambers for 45 hours and then BRDU was added into culture medium for 3 hours before experiment termination. The cultured cells were fixed using methanol for 10 min at room temperature followed by incubating with primary antibodies overnight at 4°C and then with biotinylated secondary antibodies, streptavidin-peroxidase conjugate, and the AEC chromogen following the manufacturer's instruction. Slides were counterstained with hematoxylin. Negative controls were processed without primary antibodies. For immunofluorescence analysis, PDL cells were cultured in cell culture chambers and treated with AMEL small peptides only or AMEL small peptides plus anti-ITG b1 antibody or RohA inhibitor for 24 hours as described previously. After fixation, the cells were incubated with primary anti-YAP1 antibody (Abcam) overnight at 4°C and then with FITC-labeled secondary antibodies for 30 min. images of control and treated hPDL cells were obtained using a Leica Immunofluorescence microscope.

Periodontitis Mouse Model

All experimental procedures on rodents were approved by and conducted according to the guidelines of the Institutional Animal Care and Use Committee of Texas A&M University College of Dentistry. Wild-type C57BL/6 mice at the age of 8 weeks were obtained from Charles River Laboratory (Wilmington, MA). To induce periodontitis, sutures (5-0 silk suture) were placed around left maxillary second molars for 4 weeks as described earlier (Francis et al. 2020).

Subcutaneous Implantation

After anesthetization, the back skin of mice was sheared and sterilized. Two incisions were made on the upper and lower back areas of the prepared mice. Four groups (n = 5/group) of coated collagen scaffolds (Col-con, Col-EMD, Col-hsAMEL163 and Col-hsAMEL174) were implanted into each side of the two incisions below the subcutis as described previously (Pan et al. 2013). The experiments were terminated 4 weeks after implantation.

Periodontal Implantation

Periodontitis mice were divided into 4 groups (n=5), the treatment group (Col-EMD, Col-hsAMEL163 and Col-hsAMEL174) as well as a defect control (periodontitis/Col-con). To readily access periodontitis-related bone defects, mice were subjected to gingival flap surgery. Briefly, incisions were placed from the mesial surface of the first molar to the distal surface of the third molar on the left maxilla. Full-thickness flaps were elevated, and Col-con or Col-AMEL scaffolds were applied to the surface of the exposed alveolar bone and sutured in place. Experiments were terminated 6 weeks after implantation.

Micro–Computed Tomography

Mouse left-side maxillae after 6 weeks' implantation experiment were collected and fixed. Micro–computed tomography (μCT) images from the prepared left maxillae were captured and reconstructed in 3 dimensions using a Scanco 40 μCT apparatus (Scanco Medical). Bone volume and mineral density were analyzed using a TeraRecon software package as described previously (Lu et al. 2016).

Histological Staining

Implants were deparaffinized in xylene for 3x5 min, rehydrated in a descending ethanol series (100% 3x5 min, 95% 2x5 min, 70% for 5 min, 50% for 5 min) and rinsed in deionized water for 5 min. For hematoxylin and eosin (H&E) staining, deparaffinized and rehydrated sections were dipped in hematoxylin for 5 min, placed in PBS for 5 min, dipped in eosin for 1 min, dehydrated in an ascending ethanol series (95% for 5 sec, 100% for 5 sec), and finally cleared in xylene for 5 sec. Sections were mounted with cover slips using a toluene-based mounting solution, Permount (Fischer Scientific). Masson's Trichrome staining was used to mark collagen fibers. For this procedure, deparaffinized and rehydrated sections were re-fixed in Bouin's solution (picric acid, formaldehyde, glacial acetic acid) for 1 hour at 56°C, rinsed in running tap water for 5 min, stained in Weigert's iron hematoxylin working solution (hematoxylin, 95% alcohol, 29% ferric chloride in water, distilled water, concentrated hydrochloric acid) for 10 min, rinsed in running tap water for 10 min, washed in distilled water, stained in Biebrich scarlet-acid fuchsin solution (1% aqueous Biebrich scarlet, 1% aqueous acid fuchsin, glacial acetic acid) for 15 min, washed in distilled water, differentiated in phosphomolybdic-phosphotungstic acid solution (5% phosphomolybdic acid, 5% phosphotungstic acid) for 15 min, transferred to aniline blue solution (aniline blue, glacial acetic acid, distilled water) and stained for 10 min, rinsed briefly in distilled water, differentiated in 1% acetic acid solution for 5 min, washed in distilled water and mounted with a resinous mounting medium, Histomount (Invitrogen). Collagen stained blue, nucleus stained black and muscle, cytoplasm, keratin stained red. To determine the mineralization, the sections of un-decalcified implants were stained with alizarin red as described above.

RNA extraction and quantitative real-time PCR analysis

Cells in all organisms regulate gene expression by turnover of gene transcripts (single stranded RNA): The amount of an expressed gene in a cell can be measured by the number of copies of an RNA transcript of that gene present in a sample. In order to robustly detect and quantify gene expression from small amounts of RNA, amplification of the gene transcript is necessary. The polymerase chain reaction (PCR) is a common method for amplifying DNA; for RNA-based PCR the RNA sample is first reverse-transcribed to complementary DNA (cDNA) with reverse transcriptase.

This PCR study tested for three different gene expressions. Col 1, type 1 collagen, which is abundant in bone. Col 3, type 3 collagen, that is found in connective tissues such as lung, vessel walls and skin. ItgB-1 which is a protein cell membrane transmitter.

Total RNAs were extracted from mouse dental tissues or human PDL cells using the RNeasy Plus Mini Kit (Qiagen, Germantown, MD) according to manufacturer's instructions. One microgram of RNAs was used for cDNA generation using SuperScript III (Thermo Fisher Scientific). PCR primer tested genes were listed in Table 1. Transcript levels were quantified by SYBR Green (Applied Biosystems, Foster City, CA) based Real-Time Quantitative PCR analysis on the ABI 7000 sequence detection system (Applied Biosystems). Expression levels were normalized to levels of GAPDH. Relative expression levels were calculated using the 2-DDCt method, and values were represented as the mean expression level +/- standard deviation (SD).

Protein isolation and Western Blot Analysis

Subcutaneous implants were ground under liquid nitrogen and lysed in RIPA buffer (Cell Signaling, USA) with proteinase inhibitor cocktail (Thermo, Rd, IL, USA). The mixtures were centrifuged at 4°C at the speed of 14000/min. Concentration of the proteins was evaluated by PierceTM BCA Protein Assay Kit (Thermo, Rd, IL, USA). 25 μg protein was separated on a 20% precast polyacrylamide gel (Mini-PROTEAN TGX, Bio-Rad) and transferred to a PVDF membrane, which was incubated with primary anti-ALP (SC365769, Santa Cruz, TX) RunX2 (ab75956), and iBSP (AM02057PU-S, Origene, Rockville, MD) antibodies at 4°C overnight and then with the secondary anti-rabbit IgG antibody (ab6721). The enhanced chemiluminescence reagent (PerkinElmer) was used to detect the immunoreactive bands.

Statistical analysis

Each experiment was repeated at least 3 times, and comparison of the results in each experimental group were performed by an unpaired Student's *t* test with Welch's correction for unequal variances. All calculations were performed using GraphPad Prism 6 (GraphPad Software).

3 RESULTS

Recombinant human amelogenin isomers differentially regulate the functions of human periodontal ligament stem cells.

Photographs of the BrdU assay cells were captured under microscope. BrdU is incorporated into a cell as the cell proliferates. When BrdU is taken up by the cell, the cell appears darker in color. The darker cells in this experiment represented proliferation. Each test group, including the control, demonstrated to some extent of BrdU labeling. BrdU labeling was more evident in the test groups than the control, see Figure 1. The pie charts located in Table 1 represent the percentage of proliferation among the groups. The blue part of the pie chart represents the cells that have taken up BrdU and demonstrate proliferation. The orange part of the pie chart represents the remaining PDLSC in the test group. The larger percentage of blue in the pie chart, the more that test group undergoes proliferation. rH163 represents more proliferation compared to the others.

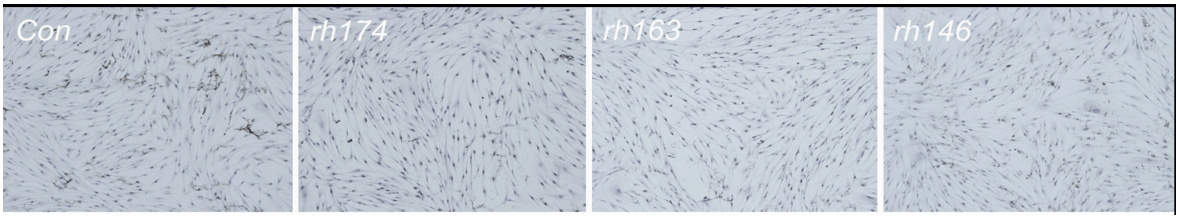

Figure 1. BrdU Incorporated Assay

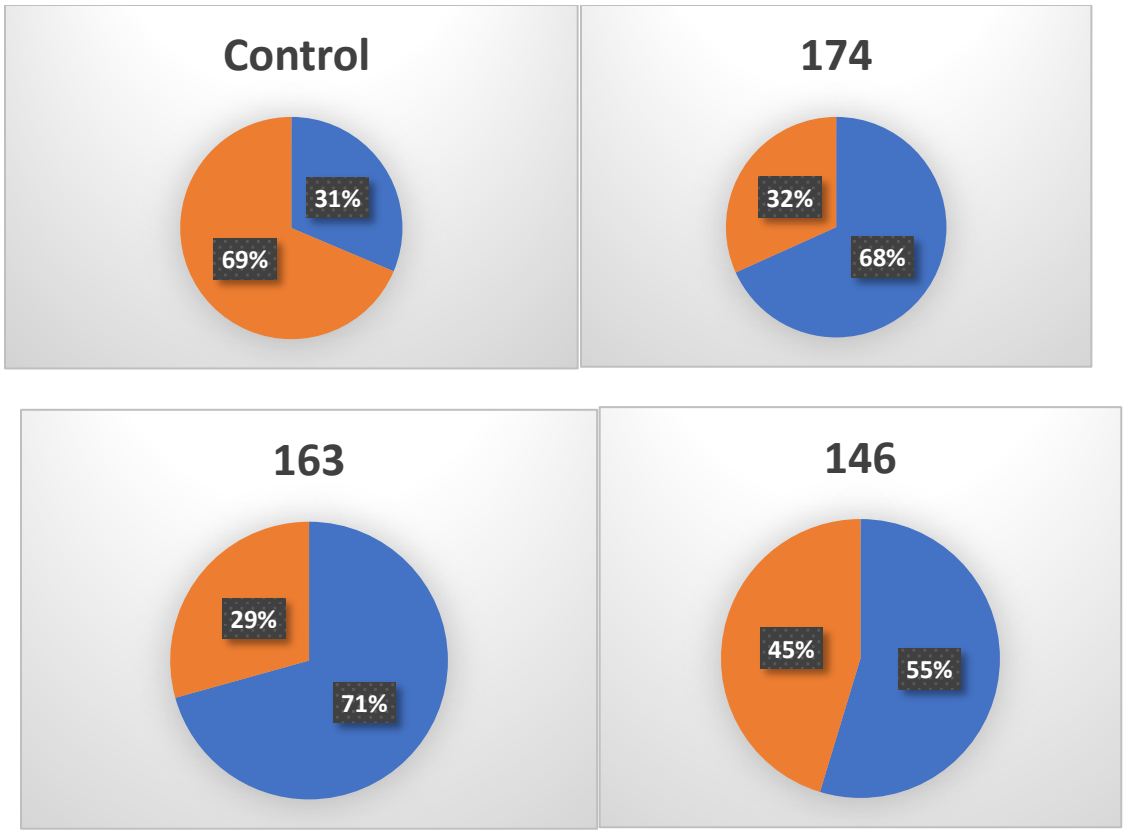

Table 1: Pie Chart of Percentile of BrdU. Blue is percent of proliferation. Orange is percent of nonproliferation.

Recombinant Human Amelogenin promoted PDLSC differentiation

In Figure 2, EDG, rH146, rH163, rH174, BSA are all darker in color than the control. rH146, rH163, and rH174 also appear darker than EMD and BSA- Bovine serum albumin, another control. In this study a darker appearing cell shows higher ALP staining, activity. More ALP activity means the cells are differentiating. The number of cells per test tube doesn't seem to be more in any of the tubes. This is to be expected.

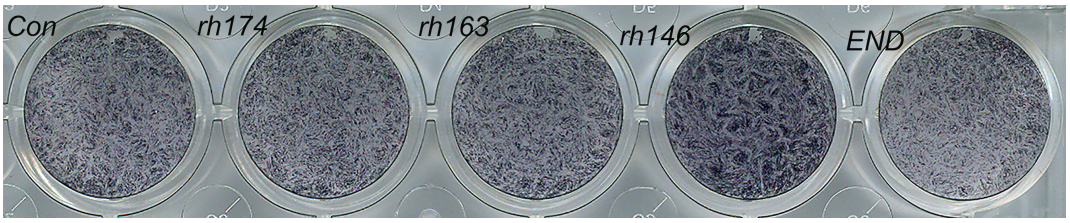

Figure 2: Alkaline Phosphatase Activity of rH Amelogenin and PDLSC

Recombinant Human Amelogenins Accelerate Cell Migration

By Day 2 faster wound healing was noted with rH163 compared to the other treatment groups and controls (Figure 3). Day 2 also demonstrated an increase in would healing with rH174 and EBD but to a lesser extent than rH163. Day 4 demonstrated complete wound migration of rH163. Almost complete wound migration was demonstrated by rH174 and EBD. rH146 had similar improved wound migration as the control. Day 5 demonstrated complete wound coverage by all of the dishes except BSA (data not shown).

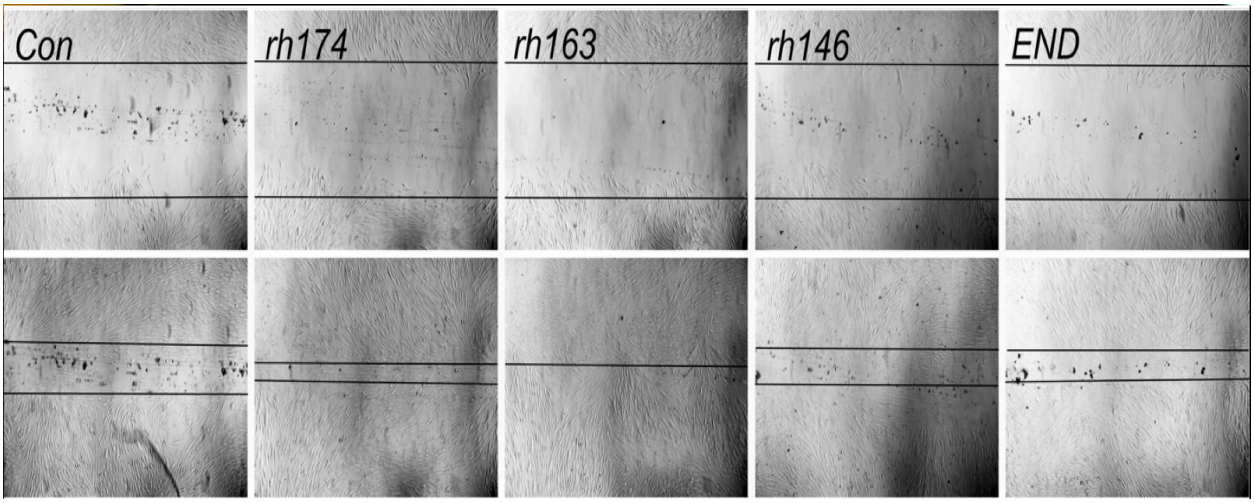

Figure 3: Cell Migration Assay of rH Amelogenins Top row is Day 1 and Bottom row is Day 4

Recombinant Amelogenins increased stem cell recruitment and new matrix formation.

After 4 weeks of implantation, cells migrated and infiltrated into the collaplug. This is to be expected to some extent even in the control. As the body heals it would naturally absorb the

collaplug and replace the space with newly formed extracellular matrix. What is important to note is the amount of cells that have infiltrated is different among the test groups and the control. All of the test groups had a larger amount of cells compared to the control. At higher magnification an extra cellular matrix is also prominent in rH163 and rH174 and to a lesser extent EMD as compared to rH146 and the control in Figure 4.

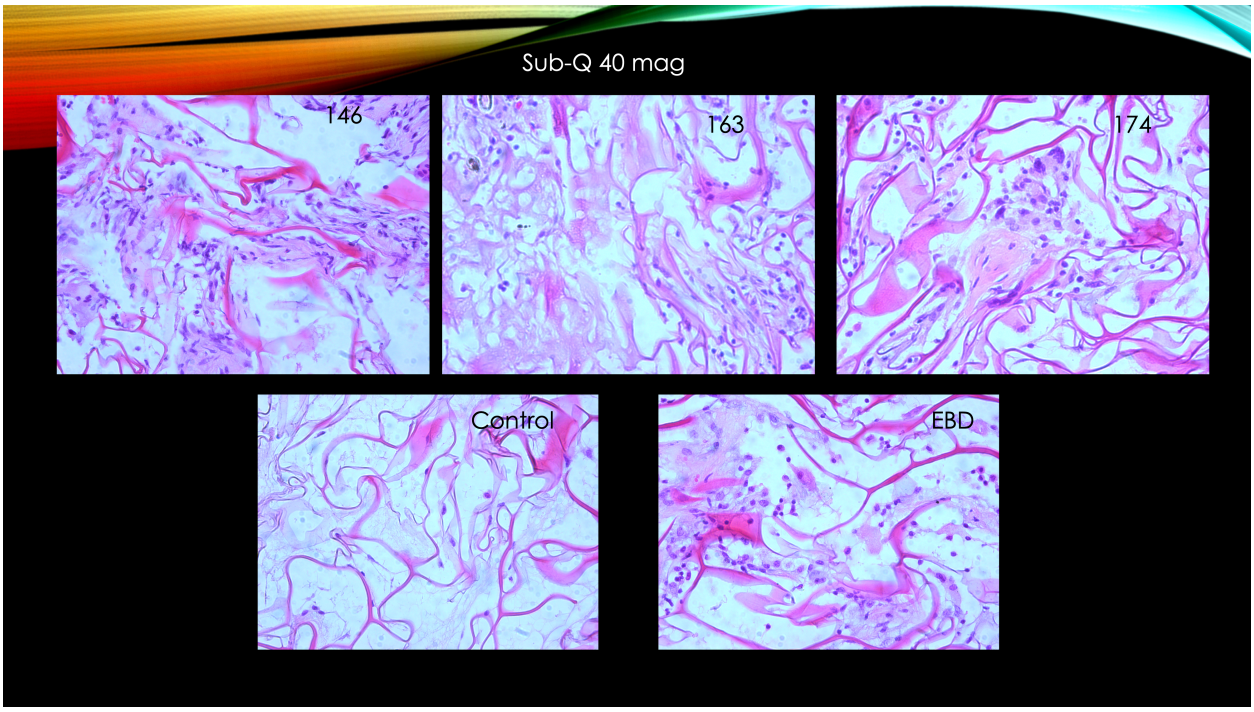

Figure 4: Subcutaneous H&E staining of rH Amelogenin

Generation of Human Amelogenin C-Terminal Fragments

After evaluating the effect of our 3 test groups rH146, rH163, and rH174, we found that our amelogenin isomers displayed different biological activity therefor we hypothesized that the C terminal end of rH163 was different than rH146 and rH173. We thought that the C-terminal difference in these isomers represented the domain of the tertiary structure of the protein. We then decided to take two fragments of the C-terminal end, one long and one short, to see if the fragments could create the same results. The exact sequence is noted in Table 2.

Human AMEL Fragment 147-63	MQPLPPMLPDLTLEAWP	Long fragment
Human AMEL Fragment 164-174	STDKTKREEVD	Short Fragment

Table 2: Sequence of Amelogenin Fragments

Amelogenin Fragments promoted PDLSC differentiation

In this study, Figure 5, a darker appearing cell shows higher ALP staining, activity. More ALP activity means the cells are differentiating. The Short fragment appears darker in color compared to the Long fragment, EMD and control. The EMD is darker in color compared to the long fragment. The Short fragment is also darker in color compared to the rH amelogenin in Figure 2.

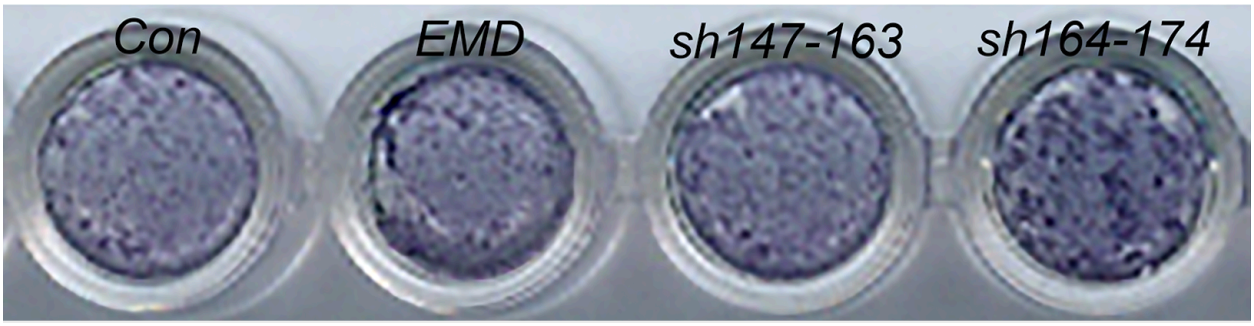

Figure 5: Alkaline Phosphatase of Amelogenin Fragments

Amelogenin Fragments promotes Mineralization and Calcium Formation

When evaluating the Alizarin Red Staining, Figure 6, the more calcium in the tissue the more mineralized the tissue. A more mineralized tissue appears a darker red compared to a tissue with minimal mineralization. Also, the fewer gaps seen in the plates the more calcium is also present in the plate.

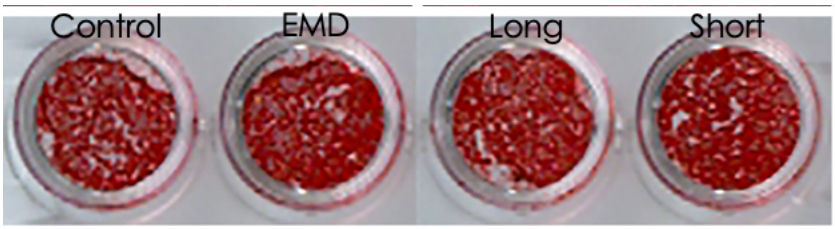

Figure 6: Alizarin Red Staining of Amelogenin Fragments

Amelogenin Fragments Accelerate Cell Migration

24 hours after initial wound experiment, the Short fragment demonstrated faster wound migration compared to the other treatment groups, Figure 7. Day 4 demonstrated complete wound migration of the Short fragment. Almost complete wound migration was demonstrated by the Long fragment. EMD and the control still had a larger wound margin at Day 4, Figure 8.

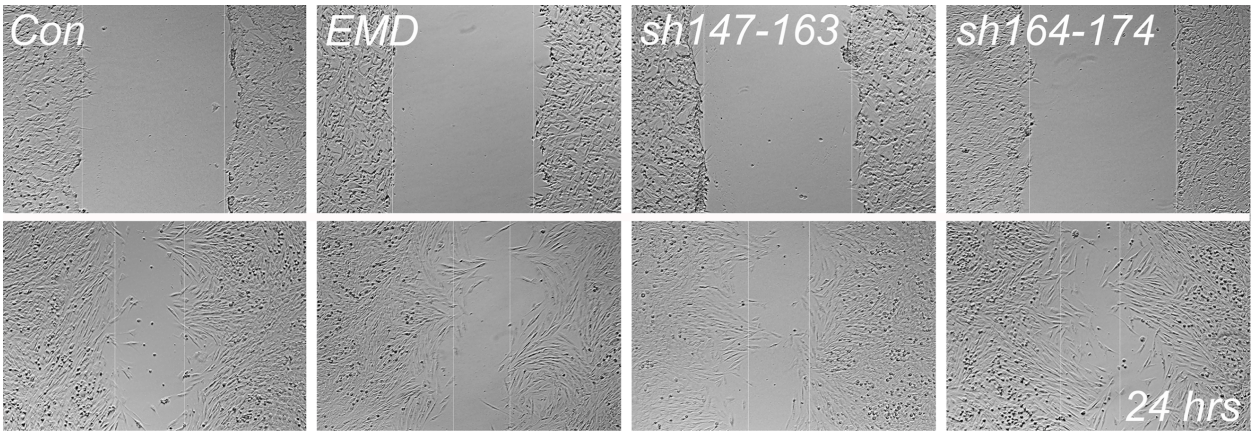

Figure 7 Cell Migration of Amelogenin Fragments, Day 0-1 Day 0- Top Row, Day 1-Bottom Row

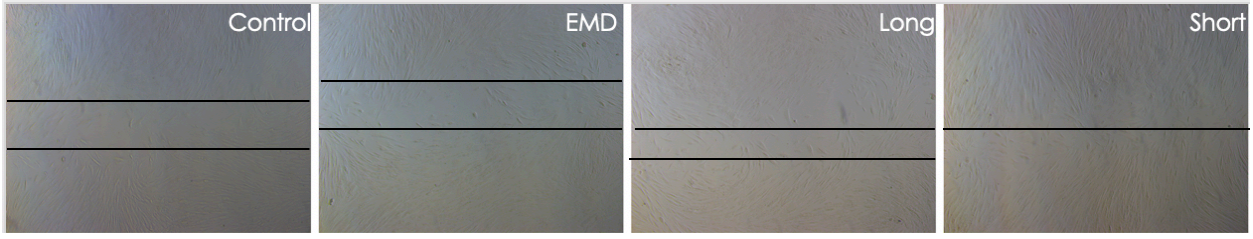

Figure 8 Cell Migration of Amelogenin Fragments, Day 4

Gene Expression of Amelogenin Fragments with the Use of Real-Time PCR

The PCR study, Figure 9, demonstrated that the Small fragment and the EMD had comparable gene expression for Col1, type 1 collagen. The Short fragment had a 2.5-fold up regulation compared to the control, in Col1, and EMD had a 2.2-fold increase compared to the control. The Long fragment was down regulated by ½ fold compared to the control. There was no significant difference between the groups when testing for Col3. All three test groups had up regulation for the ItgB-1 gene expression. The test groups with an asterisk symbolized that all three of these groups were similar in statistical significance.

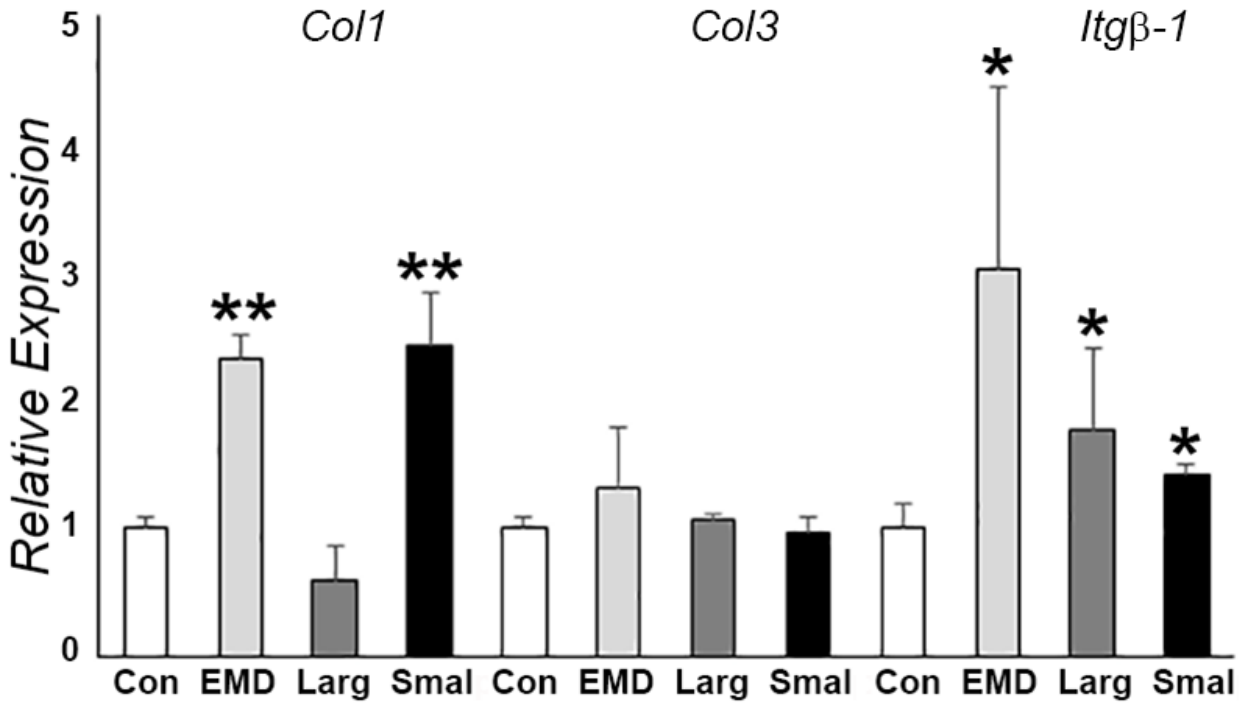

Figure 9 Real-Time PCT of Amelogenin Fragments

Amelogenin Fragments Increased Stem Cell Recruitment and New Matrix Formation

H&E staining, Figure 10, revealed a larger number of cells and more extra cellular matrix in the Small fragment subcutaneous implantation slides compared to the other groups.

The Short fragment is demonstrating new extracelluar matrix being formed and this extracellular matrix is type 1 collagen in nature. This type 1 collagen extra cellular matrix that is demonstrated in the Short fragment slide is not as well demonstrated in the other groups.

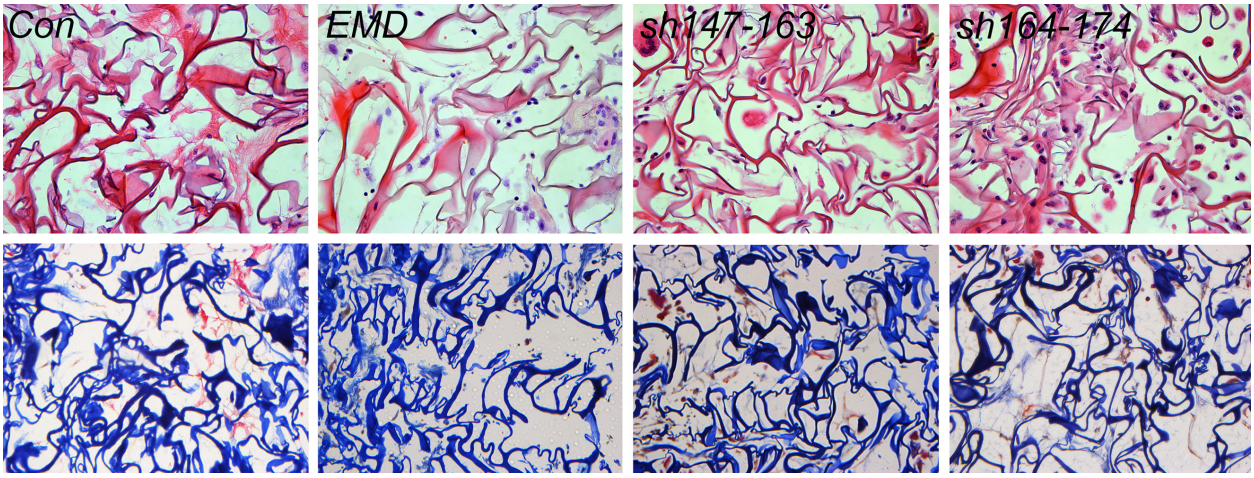

Figure 10 H&E and Masson Staining of Subcutaneous Implantation of Amelogenin Fragments

Synthesized human Amelogenin fragments restored Alveolar Bone Loss and Periodontal Ligament Regeneration in a Mouse Periodontitis Model.

Short Fragment Rescued Alveolar Bone Loss

MicroCT, Figure 11, demonstrated more bone volume and density and less exposed root with the use of the Short fragment compared to the other test groups and controls. When comparing Bone Volume to Tissue Volume, there is a greater amount of bone volume in the

Short fragment microCT than in the other test and control groups. The Long fragment demonstrated a denser bone compared to the Short fragment, EMD and control. The Short fragment had less dense bone compared to the Long fragment but denser bone compared to the EMD and the control. The number of trabecular bone cells, the thickness and the spacing between the cells were also evaluated, Tables 3, 4 and 5. What was discovered was the Short fragment had more trabecular bone cells compared to the other groups. The thickness of the bone was also more than the other groups and the spacing between the cells was less than all the other groups.

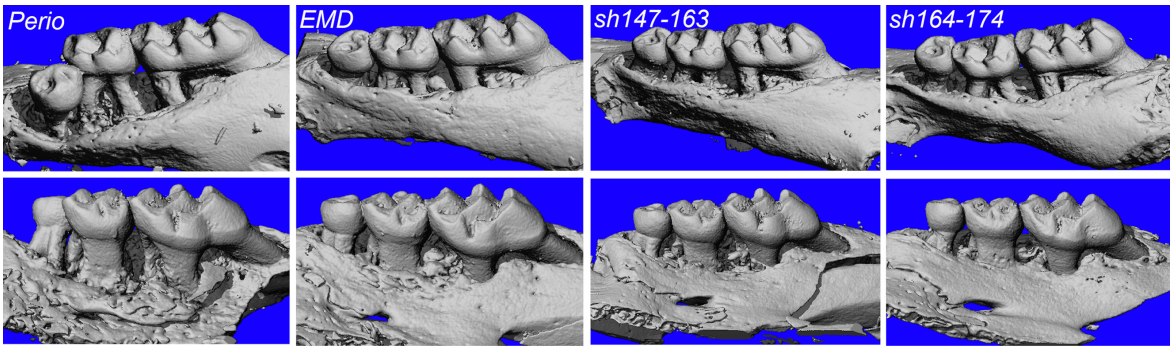

Figure 11 Week 4 Evaluation by MicroCT of Amelogenin Fragments in a Periodontitis Mouse Model.

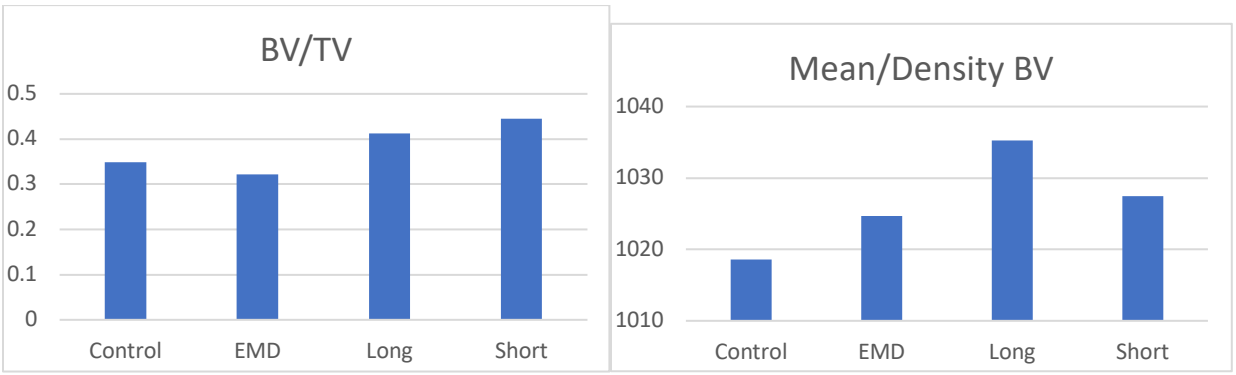

Table 3 Bone Volume and Mean Density of the Amelogenin Fragments

	Tb.Number	Tb. Thickness	Tb.Spacing
Control	**3.4413**	**0.1493**	**0.4639**
EMD	**5.417**	**0.1281**	**0.2112**
Long	**4.9134**	**0.1677**	**0.2391**
Short	**5.6501**	**0.1422**	**0.232**

Table 4 Trabecular Bone Table

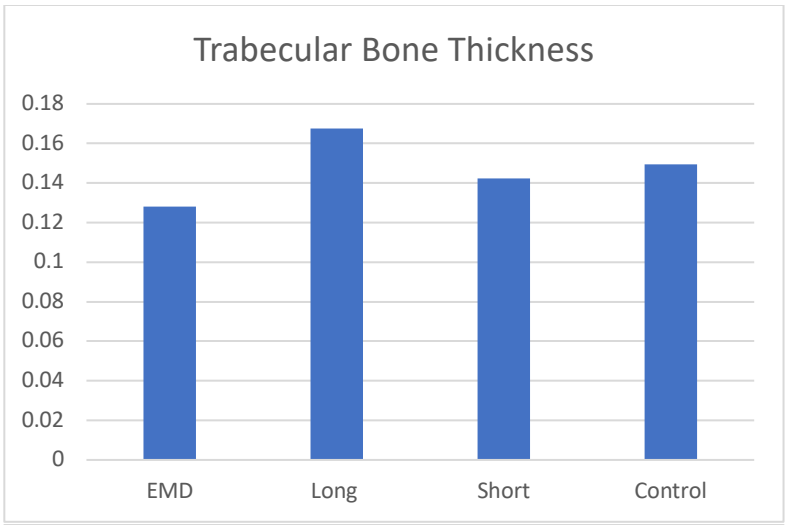

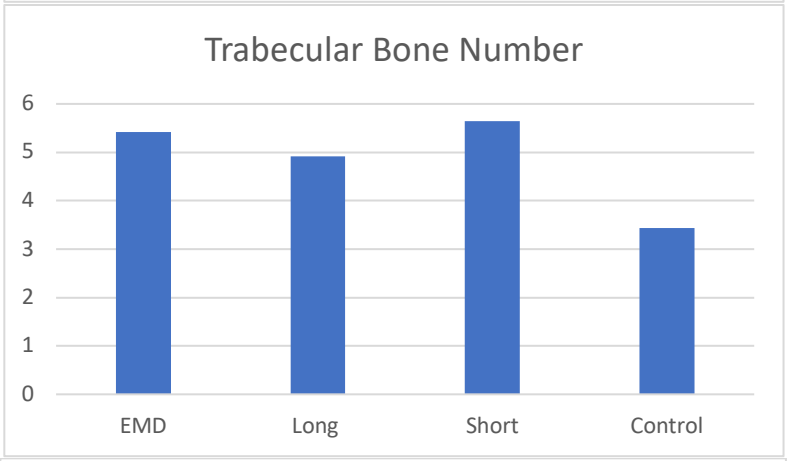

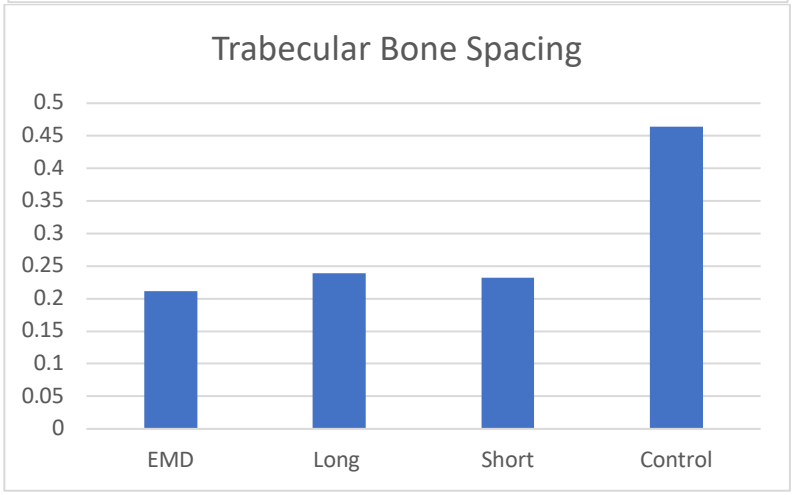

Table 5 Trabecular Bone Thickness, Number and Spacing Graphs

Short Fragment Regenerates Periodontal Defects

H&E staining in the periodontitis mouse model, Figure 12, revealed regeneration in the periodontal defect that was treated with the Short fragment. Periodontal regeneration was not demonstrated and the periodontal defect was still present on the H&E staining of the other test and control.

The Masson trichrome staining of the periodontitis mouse model demonstrated a larger amount of bone fill in the Short fragment compared to the other test and control groups. The Short fragment demonstrates a darker blue stain in the interdental area, demonstrating a more mature bone as well. This darker blue stain is not demonstrated in the other test or control groups.

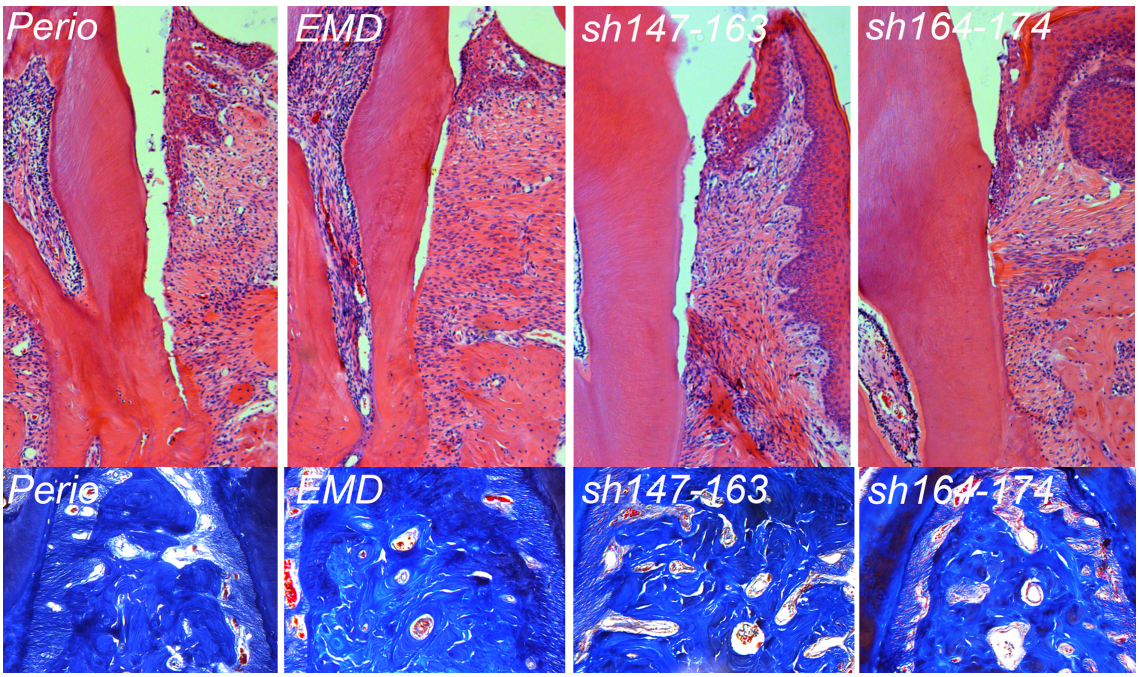

Figure 12 H&E and Masson Trichrome Staining of Amelogenin Fragments in the Periodontitis Mouse Model

Amelogenin Fragments effects on Actin Filament Assemble

In this experiment, Figure 13, the Short fragment is demonstrating more actin filaments in a parallel formation, densely packed, appearing like type 1 collagen in nature. All the other test and control groups demonstrate actin filaments but the density and formation of these filaments don't resemble type 1 collagen or bone.

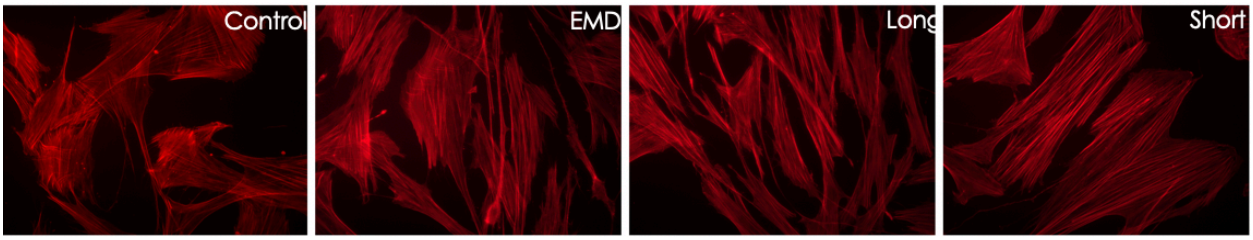

Figure 13 Phalloidin Staining of Amelogenin Fragments

sh164-174 (Short Fragment) effect on YAP protein

YAP protein localization was demonstrated using immunofluorescence staining and anti-YAP antibody, Figure 14. RhoA inhibitor or ITGB1 antibody treatment inhibited YAP nuclear translocation.

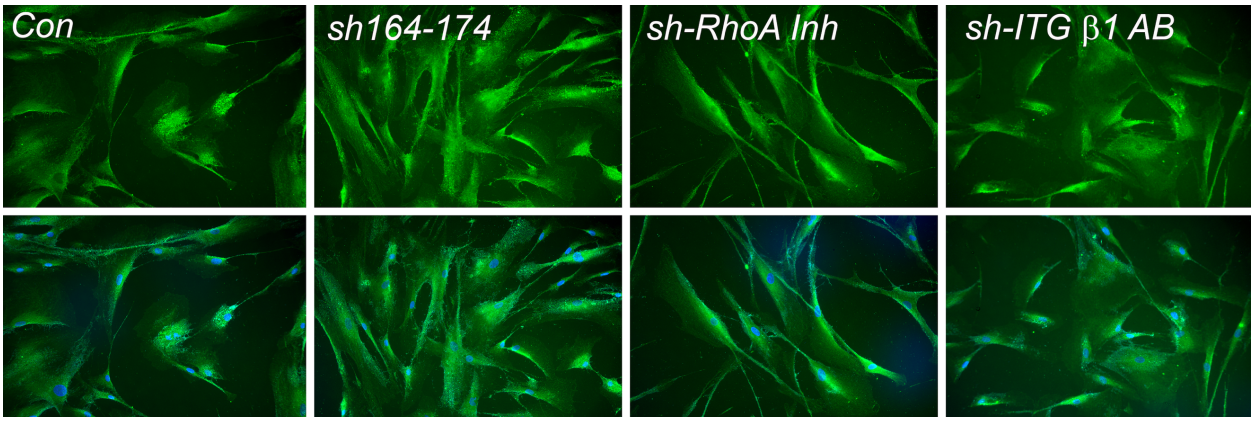

Figure 14 Enhanced Nuclear Translocation of YAP Protein in Control Group and Short Fragment Compared to That of RhoA Inhibitor or ITGB1 Antibody Treatment.

3 DISCUSSION

This study first started with examining the effects of recombinant human full-length amelogenin (rh174) along with (rh163) and (rh146) on cultured normal human periodontal cells. Alkaline phosphatase activity is a marker for osteogenic differentiation of stem cells. This particular experiment was to determine if the recombinant human amelogenins enhanced osteogenesis of PDLSC. The differentiation that would occur would demonstrate osteogenesis and differentiation. The increased darkness in appearance demonstrates a higher AP activity in these test cell tubes, thus demonstrating an increase in cell differentiation. rH174>rH146>rH163>EMD are all darker in color than the control. rH146, rH163, and rH174 also appear darker than EDG and BSA. The number of cells per test tube doesn't seem to be more in any of the tubes. This is to be expected. From this experiment, it was concluded that the rH amelogenin are in fact capable of promoting differentiation and osteogenesis.

Photographs of the BrdU assay cells were captured under microscope. The darker cells represented proliferation. The darker cells of the BrdU assay were counted, followed by the total number of cells on the image. This allowed for a percentage to be calculated. The number of proliferating cells divided by the total number of cells gave a proliferation percentage. The blue area in these graphs, Chart 1, represent the cells that demonstrated proliferation. All three rH amelogenins demonstrate an increase in proliferation. Proliferation was similar between rH174 and rH163.

rH163 demonstrated a faster would healing over its counterparts in the cell migration of rH amelogenin study. rH163>rH174>rH146=control. rH174 is the full length recombinant amelogenins. One would think that the full length amelogenin would be the peptide that stimulates the most migration. However, from this data it appears that it is not the length of the

amelogenin but the tertiary structure of the amelogenin peptides that play a larger part in cell migration. The 3D structure must be a key element in the signaling pathway of the cell.

When evaluating the H&E staining of the subcutaneous implantation of the rH amelogenin, all of the test groups had a larger number of cells compared to the control. At higher magnification an extra cellular matrix is also prominent in rH163 and rH174 and to a lesser extent EMD as compared to rH146 and the control. This extracellular matrix appears trabecular in nature. Similar to what one sees during new bone formation. What is most important to note is that the cells being recruited are local mesenchymal stem cells in nature. Amelogenin is recruiting this type of cell.

At this point in the study, we noticed the rH163 was out performing the other test and control groups in the experiment. As we discussed previously, we deciphered that the sequences and structure of these rH amelogenins must be playing a crucial role. Our thought at this point was that the domain that signals for change must be more accessible in the rH163 and rH174 than the others. After evaluating the C terminal ends of our 3 test groups rH146, rH163, and rH174, we thought that the C-terminal difference in these rH amelogenins represented the domain of the tertiary structure of the protein. We then decided to take two fragments of the C-terminal end of rH amelogenin, one long and one short, to see if the fragment could create the same results as the rH amelogenins.

The alkaline phosphatase of amelogenin fragments study demonstrated that the short fragment appears darker in color compared to the long fragment, EMD and control. The EMD is darker in color compared to the long fragment. This demonstrates that the short fragment has higher cell differentiation properties compared to EMD, Long and short fragments. The short fragment is also darker in color compared to the rH amelogenin in Figure 2. This demonstrates

that the short fragment has a higher cell differentiation property compared to the long fragment and rH amelogenin counterparts.

The PCR study demonstrated that the Short fragment and the EMD had comparable gene expression for Col1, type 1 collagen. The Short fragment had a 2.5-fold up regulation compared to the control, in Col1, and EMD had a 2.2-fold increase compared to the control. The Long fragment was down regulated by 1/2-fold compared to the control. This reveals that the Short fragment has high signaling capacity for type 1 collagen/bone compared to the other groups. There was no significant difference between the groups when testing for Col3.

All three test groups had up regulation for the ItgB-1 gene expression. The test groups with an asterisk symbolized that all three of these groups were similar in statistical significance. ITGB-1 is a cell surface receptor and associated with integrin alpha 1 and 2 to form integrin complexes. Integrins link the acting cytoskeleton with the extracellular matrix and transmit signals between the extracellular matrix and the cytoplasmic domains. Integrin dependent YAP signaling regulate cytoskeletal and local adhesion and control cell proliferation and differentiation.

H&E staining of the subcutaneous implantation of the amelogenin fragments revealed a larger number of cells and more extra cellular matrix in the Short fragment slides compared to the other groups. H&E staining in the periodontitis mouse model revealed regeneration in the periodontal defect that was treated with the Short fragment. Periodontal regeneration was not demonstrated and the periodontal defect was still present on the H&E staining of the other test groups and control.

The Masson trichrome staining of the subcutaneous implantation of the amelogenin fragments reveal new bone being extracellularly deposited with the Short fragment but not in the

other test and control groups. The Masson trichrome staining of the periodontitis mouse model demonstrated a larger amount of bone fill in the Short fragment group compared to the other test and control groups. The Short fragment demonstrates a darker blue stain in the interdental area, demonstrating a more mature bone as well. This darker blue stain is not demonstrated in the other test or control groups.

MicroCT demonstrated more bone volume and density and less exposed root with the use of the Short fragment compared to the other test groups and controls.

Through the use of animal studies, we have demonstrated that the Short fragment recruits more cells and deposits more extra cellular matrix compared to the other groups. This extra cellular matrix is collagen in nature. The collagen demonstrated in the Masson staining demonstrates a more mature bone with the use of the Short fragment application. This mature bone is not noted in the other groups. Regeneration is exhibited on the periodontitis model with the use of the Short fragment and not on any of the other group images. Regeneration is also noted with microCT evaluation with the Short fragment compared to the other test and control groups.

Phalloidin staining of amelogenin fragments demonstrated that the Short fragment is forming more actin filaments in a parallel formation, densely packed. All the other test and control groups demonstrate actin filaments but the density and formation of these filaments don't resemble the same way as in Short fragment treatment group. This is indicating that the Short fragment may affect cytoskeleton formation. Cytoskeleton is associated with cell attachment and migration.

Hippo-YAP signal blocking using RhoA inhibitor or ITGb1 antibody is one test to determine the mechanism of action of the short fragment. RhoA and ItgB1 are two different mechanisms that affect the cytoskeleton and are involved in the Hippo-YAP pathway. When either one of

these are blocked the YAP nuclear translocation was decreased. This proves that at least one mechanism of action for the Short fragment is through the Hippo-YAP signaling pathway.

4 CONCLUSION

Through invivo and invitro studies we have determined that the Short amelogenin fragment stimulates a shorter healing time and regenerates the periodontal defect compared to current FDA approved products on the market.

REFERENCES

1 Lyngstadaas, S. P., Wohlfahrt, J. C., Brookes, S. J., Paine, M. L., Snead, M. L. & Reseland, J. E. (2009) Enamel matrix proteins; old molecules for new applications. *Orthodontics and Craniofacial Research* 12, 243–253.

2 Lyngstadaas SP, Lundberg E, Ekdahl H, Andersson C, Gestrelius S. Autocrine growth factors in human periodontal ligament cells cultured on enamel matrix derivative. *J Clin Periodontol* 1991; 28: 181– 8.

3 Veis A, Tompkins K, Alvares K, Wei K, Wang L, Wang XS *et al.* Specific amelogenin gene splice products have signaling effects on cells in culture and in implants in vivo. *J Biol Chem* 2000; 275: 41263– 72.

4 Kawase T, Okuda K, Momose M, Kato Y, Yoshie H, Burns DM. Enamel matrix derivative (EMDOGAIN) rapidly stimulates phosphorylation of the MAP kinase family and nuclear accumulation of smad2 in both oral epithelial and fibroblastic human cells. *J Periodontal Res* 2001; 36: 367– 76.

5 Lagerström, Dahl, Nakahori, Nakagome, Bäckman, Landegren, and Pettersson. "A Deletion in the Amelogenin Gene (AMG) Causes X-linked Amelogenesis Imperfecta (AIH1)." *Genomics* 10.4 (1991): 971-75. Web.

6 Lyngstadaas SP, Risnes S, Sproat BS, Thrane PS, Prydz HP. A synthetic, chemically modified ribozyme eliminates amelogenin, the major translation product in developing mouse enamel in vivo. *EMBO J* 1995; 14: 5224– 9.

7 Boyan, B.D., Weesner, T.C., et al: Porcine fetal enamel matrix derivative enhances bone formation induced by demineralized freeze dried bone allografts in vivo. *J Periodontol 71:1278-1286, 2000.*

8 Warotayanont R, Zhu D, Snead ML, Zhou Y. Leucine-rich amelogenin peptide induces osteogenesis in mouse embryonic stem cells. *Biochem Biophys Res Commun* 2008; 367: 1– 6.

9 He J, Jiang J, Safavi K, Spångberg L, Zhu Q. Emdogain promotes osteoblast proliferation and differentiation and stimulates osteoprotegerin expression. *Oral Surg Oral Med Oral Pat Oral Rad Endo* 2004; 97: 239– 45.

10 Reseland JE, Reppe S, Larsen AM, Berner HS, Reinholt FP, Gautvik KM *et al.* The effect of enamel matrix derivative (EMD) on gene expression in osteoblasts. *Eur J Oral Sci* 2006; 114: 205– 11.

11 Haze A, Taylor AL, Blumenfeld A, Rosenfeld E, Leiser Y, Dafni L *et al.* Amelogenin expression in long bone and cartilage cells and in bone marrow progenitor cells. *Anat Rec* 2007; 290: 455– 60.

12 Spahr A, Lyngstadaas SP, Boeckh C, Andersson C, Podbielski A, Haller B.: Effect of the enamel matrix derivative Emdogain on the growth of periodontal pathogens in vitro. *J Clin Periodontol. 2002 Jan;29(1):62-72.*

13 E. Chen, R. Piddington, S. Decker, J. Park, Z.A. Yuan, W.R. Abrams,…, C.W. Gibson Regulation of amelogenin gene expression during tooth development Developmental Dynamics, 199 (3) (1994), pp. 189-198

14 Fincham AG, Moradian-Oldak J, Simmer JP, Sarte P, La EC, Diekwisch T *et al.* Self-assembly of a recombinant amelogenin protein generates supramolecular structures. *J Struct Biol* 1994; 112: 103– 9.

15 Gestrelius S, Andersson C, Johansson A-C, Persson E, Brodin A, Rydhag L *et al.* Formulation of enamel matrix derivative for surface coating. Kinetics and cell colonization. *J Clin Periodontol* 1997; 24: 678– 84.

16 Suzuki S, Nagano T, Yamakoshi Y, Gomi K, Arai T, Fukae M *et al.* Enamel matrix derivative gel stimulates signal transduction of BMP and TGF-ß. *J Dent Res* 2005; 84: 510– 4.

17 Yamamichi, Kensuke, Takao Fukuda, Terukazu Sanui, Kyosuke Toyoda, Urara Tanaka, Yuki Nakao, Karen Yotsumoto, Hiroaki Yamato, Takaharu Taketomi, Takeshi Uchiumi, and Fusanori Nishimura. "Amelogenin Induces M2 Macrophage Polarisation via PGE2/cAMP Signalling Pathway." *Archives of Oral Biology* 83 (2017): 241-51. Web.

18 Li, Jie, Yan-Ping Zhang, Robert S. Kirsner, Vidal, Sergio, and Kovacs, Kalman. "Angiogenesis in Wound Repair: Angiogenic Growth Factors and the Extracellular Matrix." *Microscopy Research and Technique* 60.1 (2003): 107-14. Web.

19 Kunimatsu, R., Yoshimi, Y., Awada, T., & Tanimoto, K. (2018). Effects of human full-length amelogenin on the proliferation of human osteoblasts. *Biomedical Research, 29*(12). doi:10.4066/biomedicalresearch.29-18-641

20 Miron RJ, Dard M, Weinreb M. Enamel matrix derivative, inflammation and soft tissue wound healing. J Periodontal Res. 2015 Oct;50(5):555-69. doi: 10.1111/jre.12245. Epub 2014 Nov 23. PMID: 25418917.

21 Miron RJ, Sculean A, Cochran DL, Froum S, Zucchelli G, Nemcovsky C, Donos N, Lyngstadaas SP, Deschner J, Dard M, Stavropoulos A, Zhang Y, Trombelli L, Kasaj A, Shirakata Y, Cortellini P, Tonetti M, Rasperini G, Jepsen S, Bosshardt DD. Twenty years of enamel matrix derivative: the past, the present and the future. J Clin Periodontol. 2016 Aug;43(8):668-83. doi: 10.1111/jcpe.12546. Epub 2016 May 28. PMID: 26987551.

22 Dey, Anwesha, Varelas, Xaralabos, and Guan, Kun-Liang. "Targeting the Hippo Pathway in Cancer, Fibrosis, Wound Healing and Regenerative Medicine." *Nature Reviews. Drug Discovery* 19.7 (2020): 480-94. Web.

23 Plouffe, Steven W, Meng, Zhipeng, Lin, Kimberly C, Lin, Brian, Hong, Audrey W, Chun, Justin V, and Guan, Kun-Liang. "Characterization of Hippo Pathway Components by Gene Inactivation." *Molecular Cell* 64.5 (2016): 993-1008. Web.

APPENDEX

FIGURES

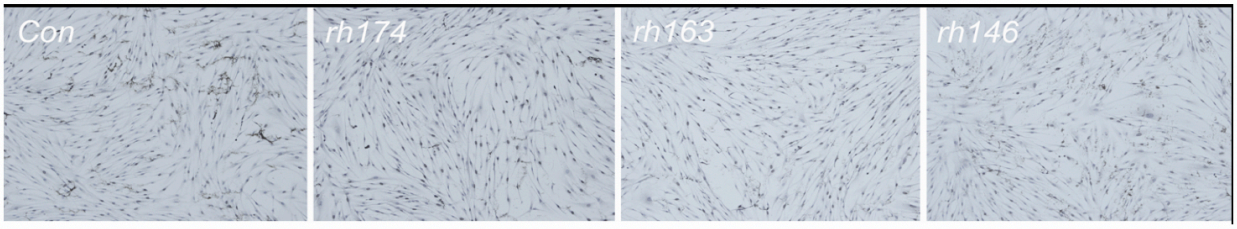

Figure 1. BrdU Incorporated Assay

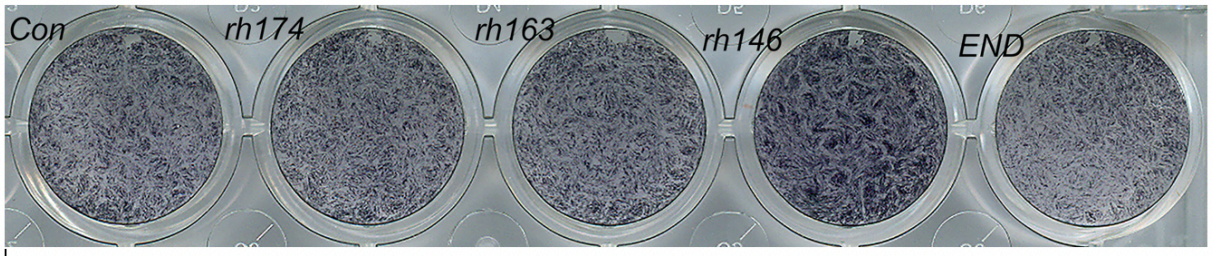

Figure 2: Alkaline Phosphatase Activity of rH Amelogenin and PDLSC

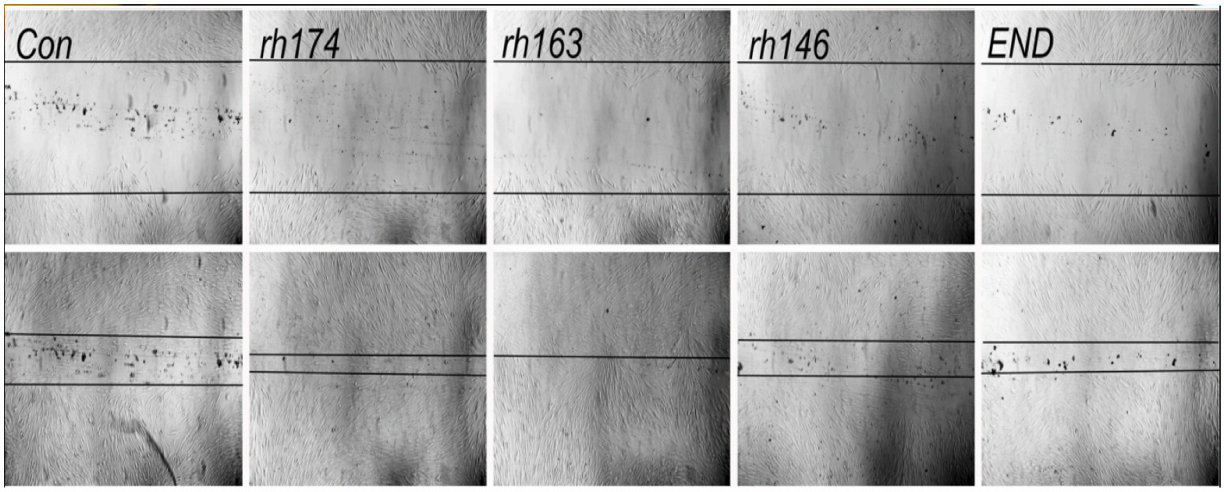

Figure 3: Cell Migration Assay of rH Amelogenins Top row is Day 1 and Bottom row is Day 4

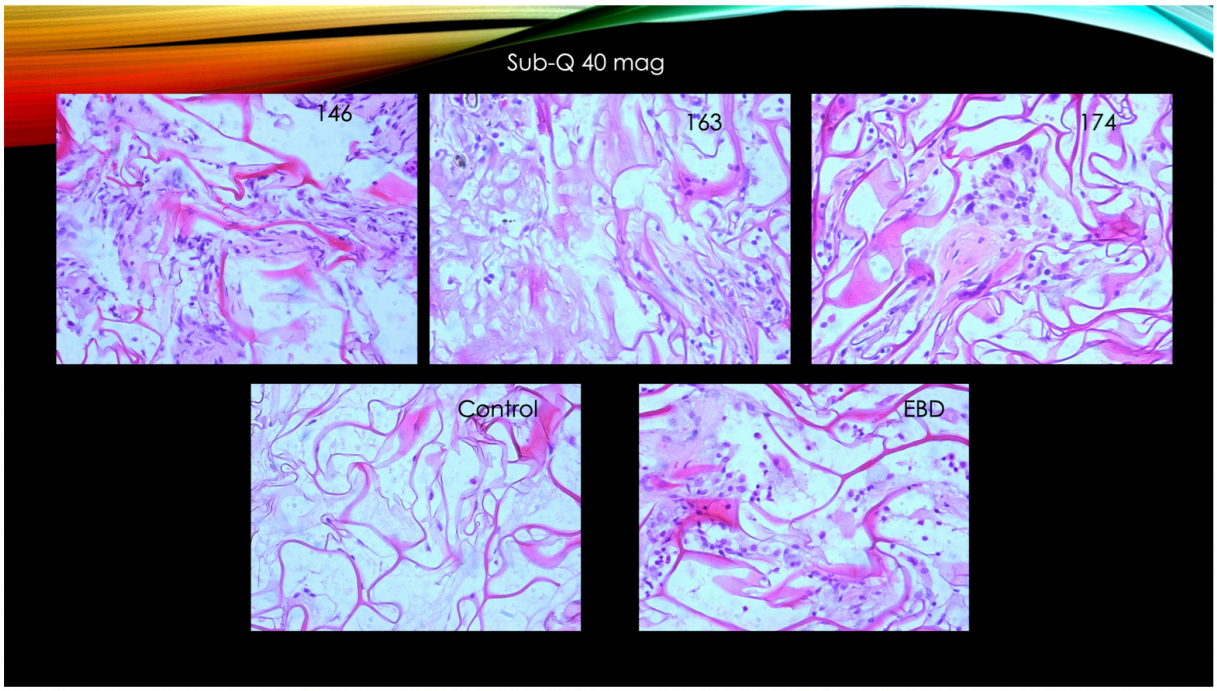

Figure 4: Subcutaneous H&E staining of rH Amelogenin

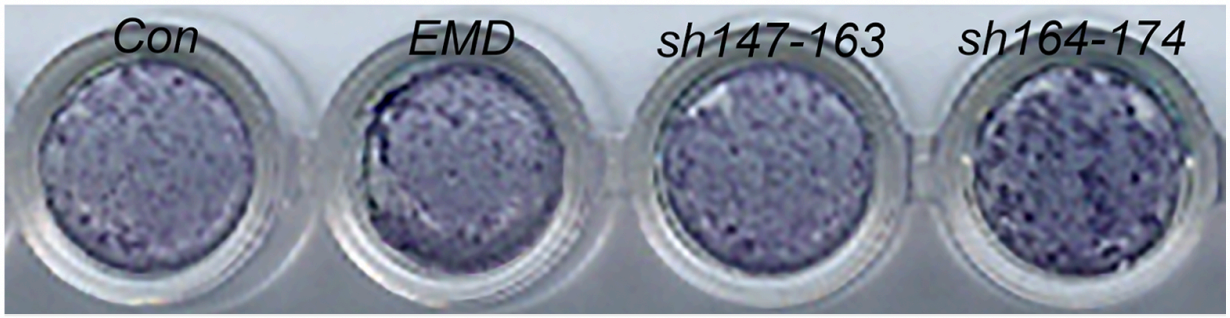

Figure 5: Alkaline Phosphatase of Amelogenin Fragments

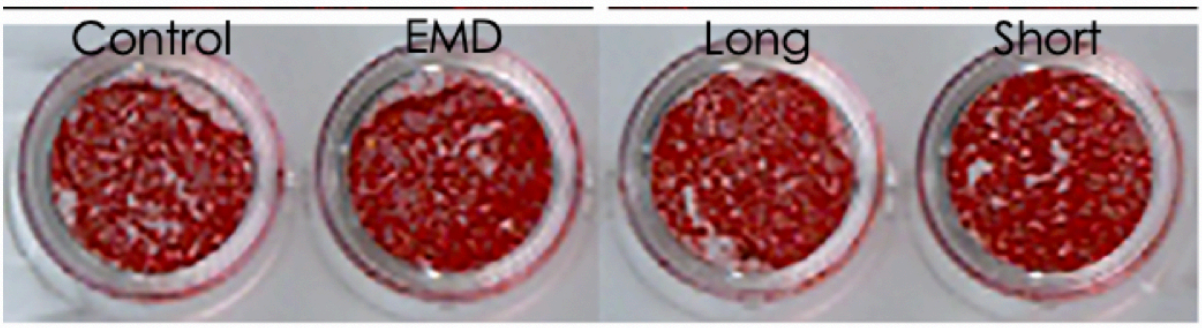

Figure 6: Alizarin Red Staining of Amelogenin Fragments

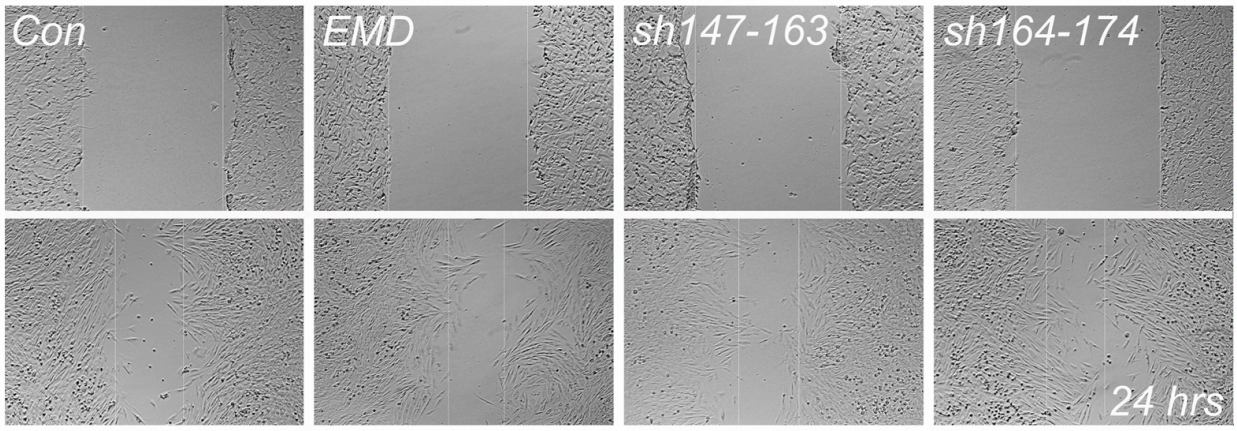

Figure 7 Cell Migration of Amelogenin Fragments, Day 0-1 Day 0- Top Row, Day 1-Bottom Row

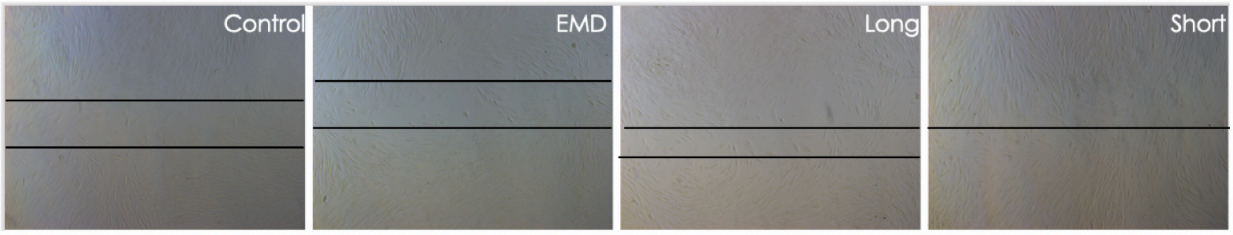

Figure 8 Cell Migration of Amelogenin Fragments, Day 4

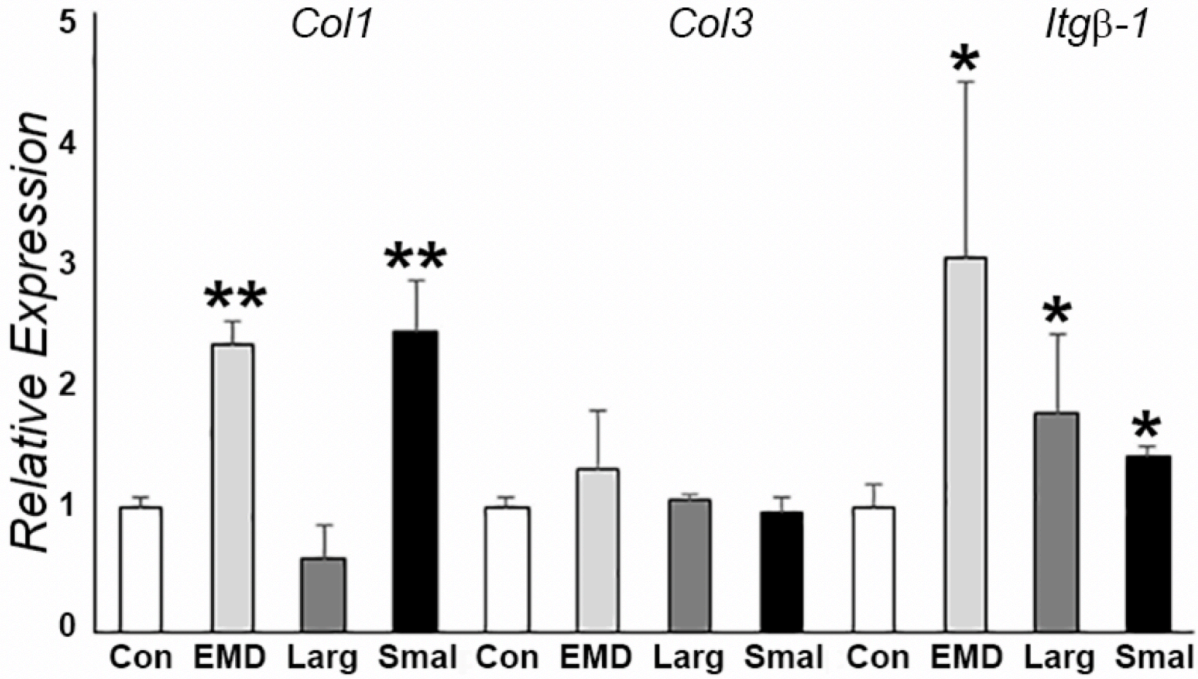

Figure 9 Real-Time PCT of Amelogenin Fragments

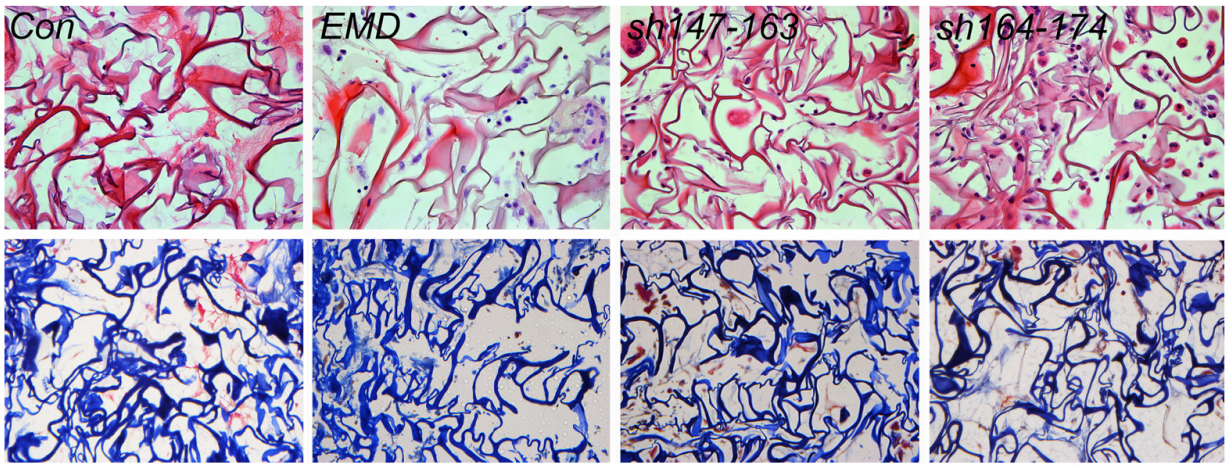

Figure 10 H&E and Masson Staining of Subcutaneous Implantation of Amelogenin Fragments

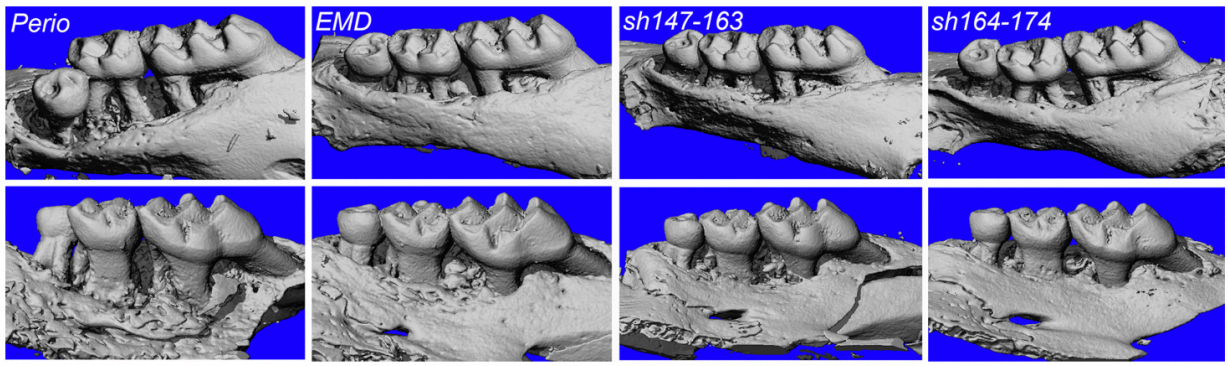

Figure 11 Week 4 Evaluation by MicroCT of Amelogenin Fragments in a Periodontitis Mouse Model.

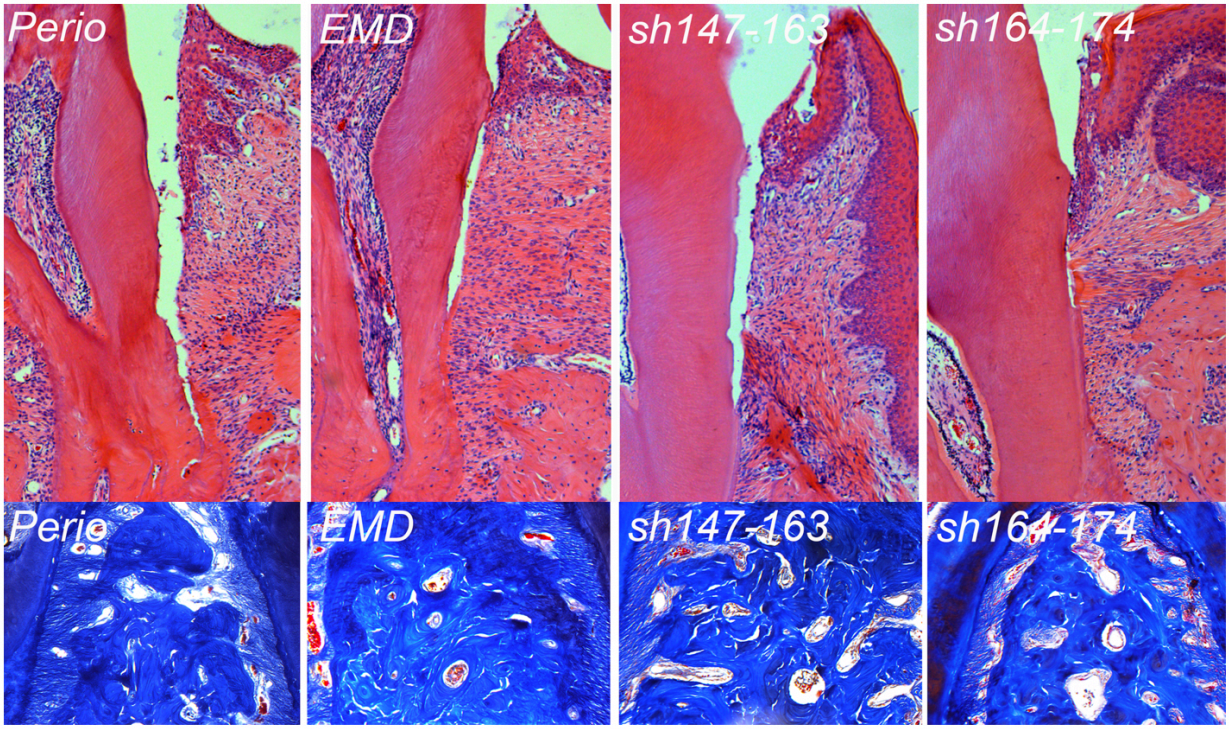

Figure 12 H&E and Masson Trichrome Staining of Amelogenin Fragments in the Periodontitis Mouse Model

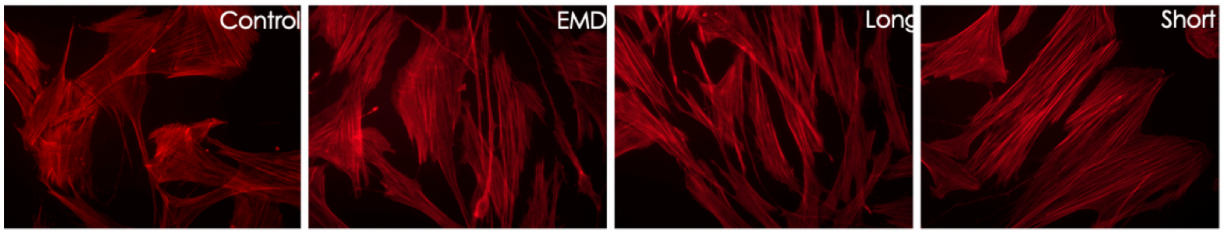

Figure 13 Phalloidin Staining of Amelogenin Fragments

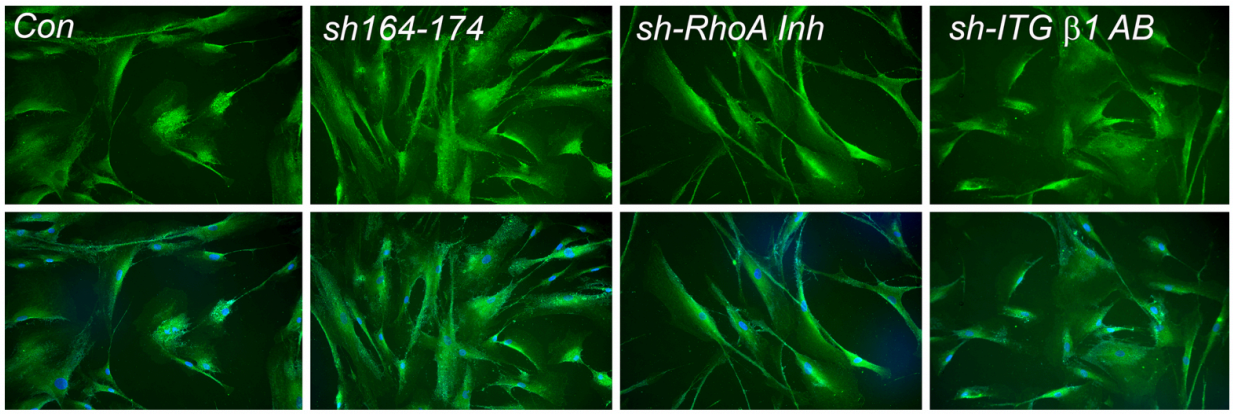

Figure 14 Enhanced Nuclear Translocation of YAP Protein in Control Group and Short Fragment Compared to That of RhoA Inhibitor or ITGB1 Antibody Treatment.

TABLES

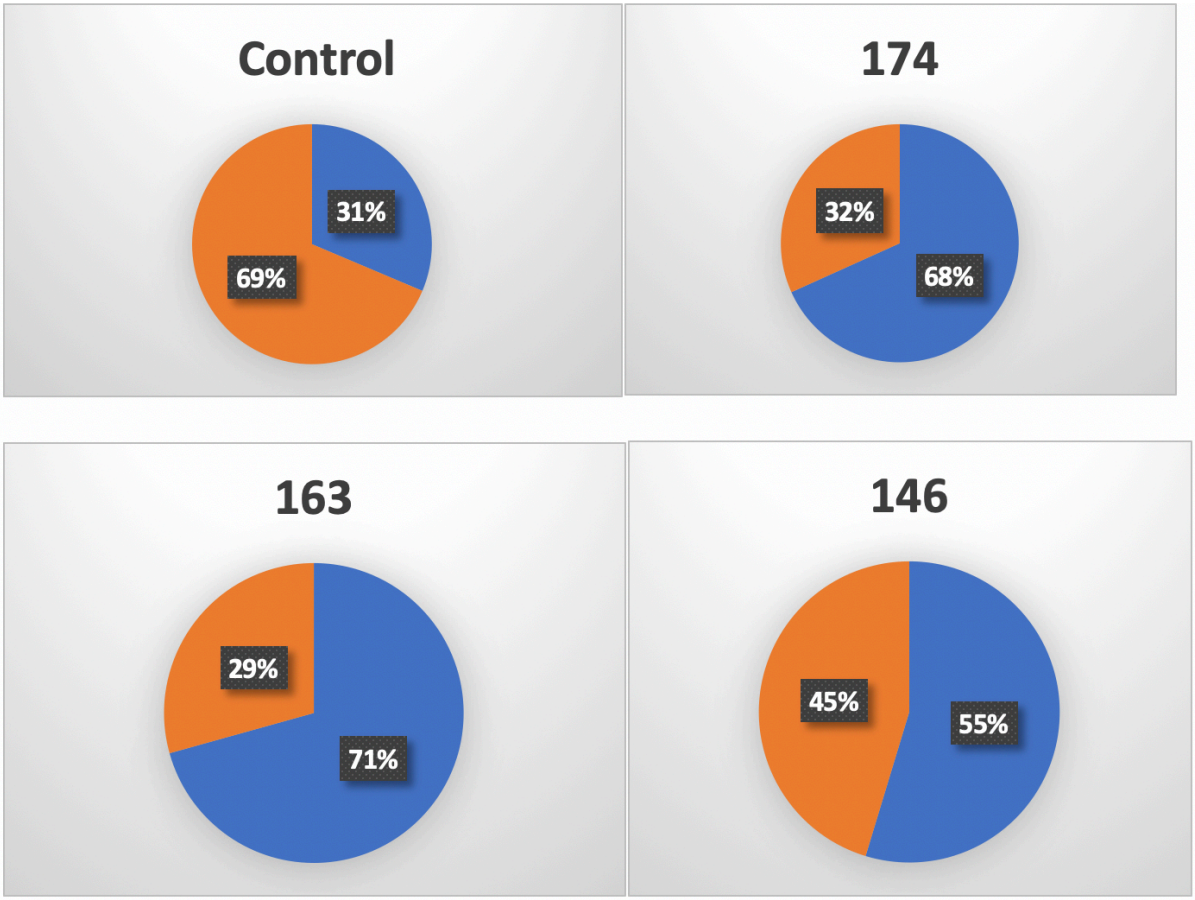

Table 1: Pie Chart of Percentile of BrdU. Blue is percent of proliferation. Orange is percent of nonproliferation.

Human AMEL Fragment 147-63	MQPLPPMLPDLTLEAWP	Long fragment
Human AMEL Fragment 164-174	STDKTKREEVD	Short Fragment

Table 2: Sequence of Amelogenin Fragments

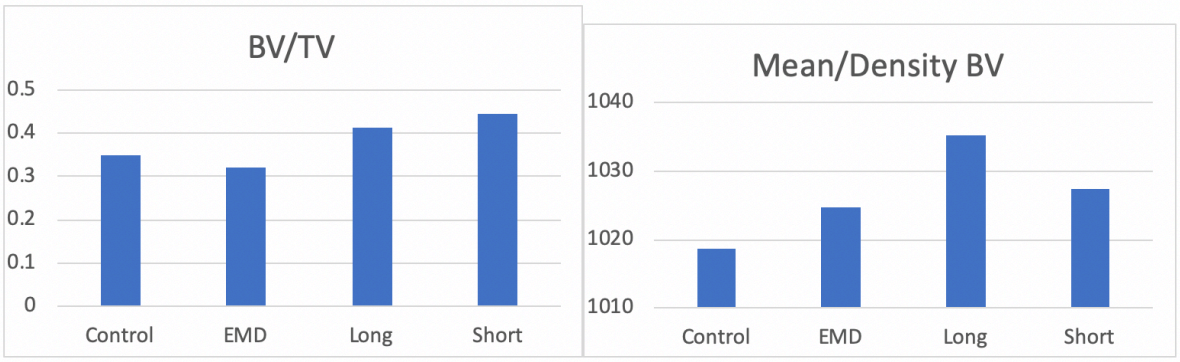

Table 3 Bone Volume and Mean Density of the Amelogenin Fragments

	Tb.Number	Tb. Thickness	Tb.Spacing
Control	**3.4413**	**0.1493**	**0.4639**
EMD	**5.417**	**0.1281**	**0.2112**
Long	**4.9134**	**0.1677**	**0.2391**
Short	**5.6501**	**0.1422**	**0.232**

Table 4 Trabecular Bone Table

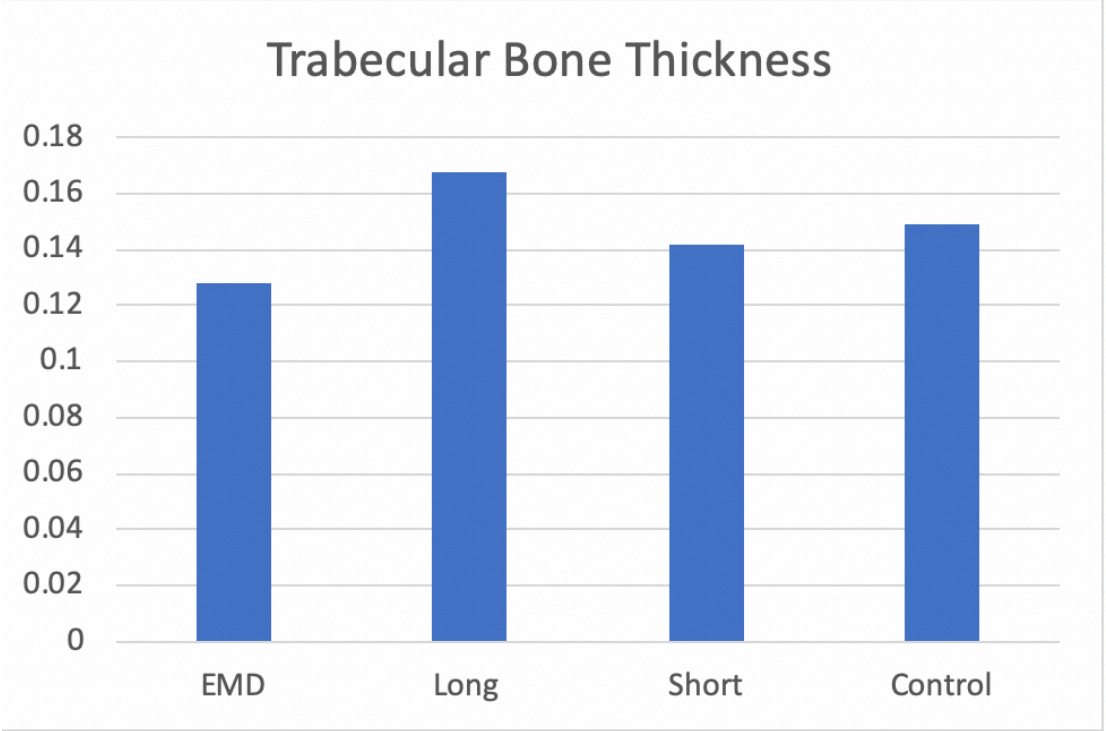
Trabecular Bone Thickness
0.18
0.16
0.14
0.12
0.1
0.08
0.06
0.04
0.02
0
EMD
Long
Short
Control

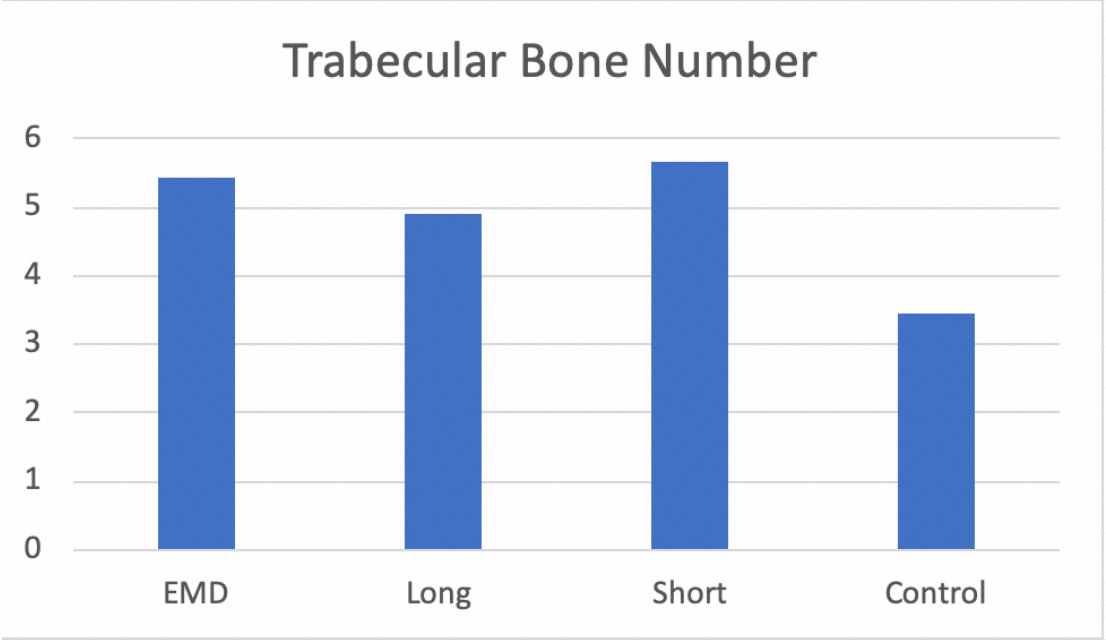
Trabecular Bone Number
6
5
4
3
2
1
0
EMD
Long
Short
Control

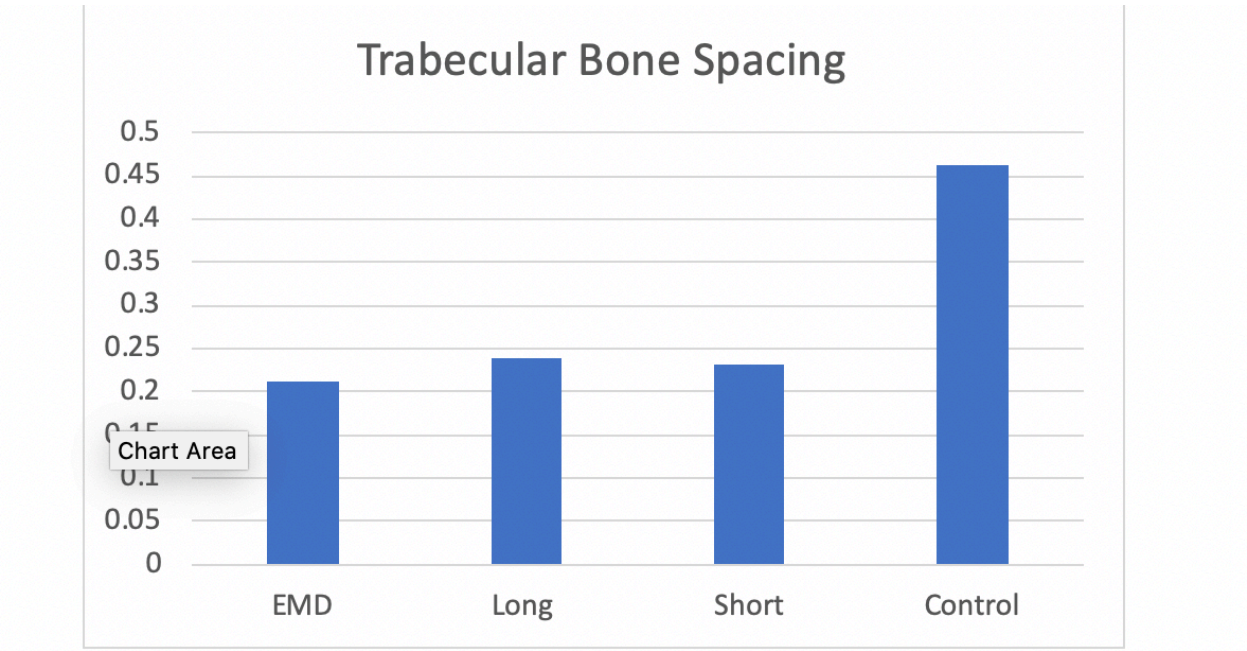

Table 5 Trabecular Bone Thickness, Number and Spacing Graphs